BE MORE DIVERSE THAN THE MOST DIVERSE: ONLINE SELECTION OF DIVERSE MIXTURES OF GENERATIVE MODELS

Anonymous authors
Paper under double-blind review

ABSTRACT

The availability of multiple training algorithms and architectures for generative models requires a selection mechanism to form a single model over a group of well-trained generation models. The selection task is commonly addressed by identifying the model that maximizes an evaluation score based on the diversity and quality of the generated data. However, such a best-model identification approach overlooks the possibility that a mixture of available models can outperform each individual model. In this work, we explore the selection of a mixture of multiple generative models and formulate a quadratic optimization problem to find an optimal mixture model achieving the maximum of kernel-based evaluation scores including kernel inception distance (KID) and Rényi kernel entropy (RKE). To identify the optimal mixture of the models using the fewest possible sample queries, we propose an online learning approach called *Mixture Upper Confidence Bound (Mixture-UCB)*. Specifically, our proposed online learning method can be extended to every convex quadratic function of the mixture weights, for which we prove a concentration bound to enable the application of the UCB approach. We prove a regret bound for the proposed Mixture-UCB algorithm and perform several numerical experiments to show the success of the proposed Mixture-UCB method in finding the optimal mixture of text-based and image-based generative models.

1 INTRODUCTION

The rapid advancements in generative modeling have created a need for mechanisms to combine multiple well-trained generative models, each developed using different algorithms and architectures, into a single unified model. A common approach for creating such a unified model is to evaluate assessment scores that quantify the diversity and quality of the generated data and then select the model with the highest score. This best-model identification strategy has been widely adopted for the selection of generative models across various domains, including image, text, audio, and video generation.

Existing model selection frameworks typically perform an offline selection, where they have access to a sufficiently large number of samples from each generative model and estimate the evaluation score based on these samples. However, in many practical scenarios, generating a large sample set from sub-optimal models can be computationally costly, especially if the evaluator can identify their lack of optimality using fewer samples. In such cases, the evaluator can adopt an online learning approach and frame the problem as a multi-armed bandit (MAB) task. In each round, we choose a model to generate one sample, where the choice of model is based on previous samples. This allows us to quickly identify obviously sub-optimal models and avoid them, reducing the cost of generating from sub-optimal models.

An existing approach is *successive halving* (Karnin et al., 2013; Jamieson & Talwalkar, 2016; Chen & Ghosh, 2024),[1] where the models are evaluated using a fixed budget, the worst half of the models

[1]Jamieson & Talwalkar (2016) focused on applying successive halving on hyperparameter optimization for supervised learning, whereas Chen & Ghosh (2024) focused on generative models using maximum mean discrepancy (Gretton et al., 2012) as the score.

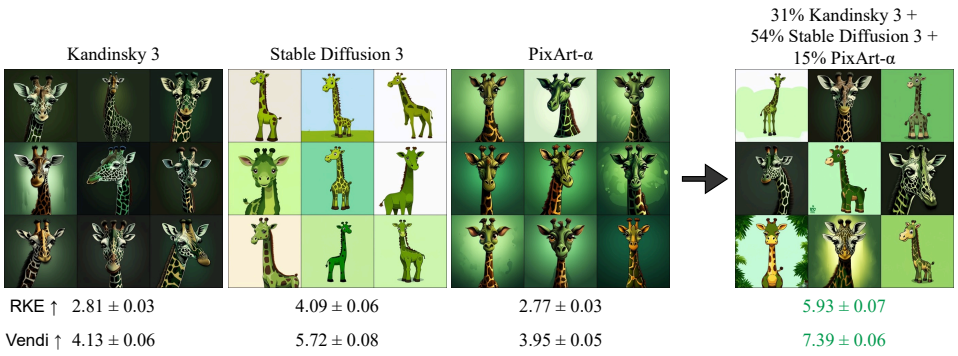

Figure 1: Visual comparison of the diversity across individual arms and the optimal mixture for images generated using models Kandinsky 3, Stable Diffusion 3-medium, and PixArt-α the prompt "Dark green giraffe, detailed, cartoon style".

are removed, and we repeat the process until one model is left. Also, the recent work by Hu et al. (2024) attempts to solve the online model selection problem using an upper confidence bound (UCB) method to identify the generative model with the highest evaluation score. The numerical results of Hu et al. (2024) indicate the effectiveness of MAB algorithms in reducing sample generation costs from sub-optimal models.

On the other hand, when the model selection task is handled by an online learning algorithm, the algorithm may choose different models at different iterations, resulting in generated data that follow a mixture of the distributions of these generative models. Note that in a standard MAB algorithm, the goal is to eventually converge to a single arm. Successive halving (Karnin et al., 2013; Jamieson & Talwalkar, 2016; Chen & Ghosh, 2024) and the standard UCB algorithm adopted by Hu et al. (2024) will ultimately select only one generative model after a sufficient number of iterations. However, the diversity scores of the generated data could be higher when the sample generation follows a mixture of models rather than a single model. This observation leads to the following question: could the diversity of generated data be improved by applying MAB algorithms to multiple generative models, if the algorithm aims to find the best mixture of the models?

In this work, we aim to address the above question by finding the optimal mixture $\sum_{i=1}^{m} \alpha_i P_i$ of m generative models with distributions $P_1, \ldots, P_m$, which would produce a higher evaluation score compared to each individual model. Specifically, we focus on addressing this task in an online learning setting, where we pick a model to generate a sample at each round. To address this problem and develop an MAB algorithm to find the best mixture model, we concentrate on evaluation scores that are quadratic functions of the generated data. As we show in this work, formulating the optimization problem for a quadratic score function results in a quadratic online convex optimization problem that can be efficiently solved using the online gradient descent algorithm. More importantly, we establish a concentration bound for the quadratic function of the mixture weights, which enables us to extend the UCB algorithm for the online selection of the mixture weights.

Specifically, we focus on evaluation scores that reduce to a quadratic function of the generative model's distribution, including the kernel-based Maximum Mean Discrepancy (MMD) (Gretton et al., 2012), Kernel Inception Distance (KID) (Bińkowski et al., 2018) and Rényi Kernel Entropy (RKE) (Jalali et al., 2023) scores, as well as the quality-measuring Precision (Sajjadi et al., 2018; Kynkäänniemi et al., 2019) and Density (Naeem et al., 2020) scores, which are linear functions of the generative distribution. Among these scores, RKE provides a reference-free entropy function for assessing the diversity of generated data, making it suitable for quantifying the variety of generated samples. Our mixture-based online learning framework can therefore be applied to find the mixture model with the maximum RKE-based diversity score. Additionally, we can consider a linear combination of RKE with the Precision, Density, or KID quality scores to identify a mixture of models that offers the best trade-off between quality and diversity.

We perform several numerical experiments to test the application of our proposed Mixture-UCB approach in comparison to the Vanilla-UCB and One-Arm Oracle approaches that tend to generate samples from only one of the available generative models. Our numerical results indicate that the Mixture-UCB algorithms can generate samples with higher RKE diversity scores, and tends to gen-

erate samples from a mixture of several generative models when applied to image-based generative models. Also, we test the performance of Mixture-UCB on the KID, Precision, and Density scores, which similarly result in a higher score value for the mixture model found by the Mixture-UCB algorithm. We implement the Mixture-UCB by solving the convex optimization sub-problem at every iteration and also by applying the online gradient descent algorithm at every iteration. In our experiments, both implementations result in satisfactory results and can improve upon learning strategies tending to select only one generative model. Here is a summary of this work's contributions:

- Studying the selection task for mixtures of multiple generative models to improve the diversity of generated samples (Section 4).
- Proposing an online learning framework to address the mixture selection task for quadratic score functions (Section 5).
- Developing the Mixture-UCB-CAB and Mixture-UCB-OGD algorithms to solve the formulated online learning problem (Sections 5.1, 5.2).
- Proving a regret bound for Mixture-UCB-CAB which shows the convergence of Mixture-UCB-CAB to the optimal mixture (Theorem 2).
- Presenting numerical results on the improvements in the diversity of generated data by the online selection of a mixture of the generation models (Section 6, Appendix 8.3).

2 Related Work

Assessment of Generative Models. The evaluation of generative models has been extensively studied, with a focus on both diversity and quality of generated images. Reference-free metrics such as Rényi Kernel Entropy (RKE) (Jalali et al., 2023) and VENDI (Friedman & Dieng, 2023) measure diversity without relying on ground-truth, while reference-based metrics such as Recall (Kynkäänniemi et al., 2019) and Coverage (Naeem et al., 2020) assess diversity relative to real data. For image quality evaluation, Density and Precision metrics (Naeem et al., 2020; Kynkäänniemi et al., 2019) provide measures based on alignment with a reference distribution. The Wasserstein distance (Arjovsky et al., 2017) and Fréchet Inception Distance (FID) (Heusel et al., 2018) approximate the distance between real and generated datasets, while Kernel Inception Distance (KID) (Bińkowski et al., 2018) uses squared maximum mean discrepancy for a kernel-based comparison of distributions.

Multi-Armed Bandit Algorithms. The Multi-Armed Bandit (MAB) problem is a foundational topic in reinforcement learning, where an agent aims to maximize rewards from multiple options (arms) with initially unknown reward distributions (Lai & Robbins, 1985; Thompson, 1933). The Upper Confidence Bound (UCB) algorithm (Agrawal, 1995a; Auer, 2003; Bubeck & Cesa-Bianchi, 2012) is a widely adopted method for addressing the MAB problem, where uncertainty about an arm's reward is replaced by an optimistic estimate. In generative models, optimism-based bandits have been applied to efficiently identify models with optimal Fréchet Inception Distance (FID) or Inception Score while minimizing data queries (Hu et al., 2024). A special case of MAB, the continuum-armed bandit (CAB) problem (Agrawal, 1995b), optimizes a function over continuous inputs, and has been applied to machine learning tasks such as hyperparameter optimization (Feurer & Hutter, 2019; Li et al., 2018). Recent research explores CABs under more general smoothness conditions like Besov spaces (Singh, 2021), while other works have focused on regret bounds and Lipschitz conditions (Kleinberg, 2004; Kleinberg et al., 2019; Bubeck et al., 2008).

Another related reference is informational multi-armed bandits (Weinberger & Yemini, 2023), which extends UCB to maximizing the Shannon entropy of a discrete distribution, which is also a metric of diversity. In comparison, the algorithms in this paper can minimize the expectation of any quadratic positive semidefinite function, which not only covers the order-2 Rényi entropy for discrete distributions, but also includes the Rényi Kernel Entropy applicable to continuous data. Since the outputs of generative models are generally continuous, (Weinberger & Yemini, 2023) is not applicable here.

3 Preliminaries

We review several kernel-based performance metrics of generative models.

3.1 RÉNYI KERNEL ENTROPY

The *Rényi Kernel Entropy* (Jalali et al., 2023) of the distribution P, which measures the diversity of the modes in P, is given by $\log(1/\mathbb{E}_{X,X' \overset{\text{iid}}{\sim} P}[k^2(X, X')])$, where k is a positive definite kernel.[2]

Taking the exponential of the Rényi Kernel Entropy, we have the *RKE mode count* $1/\mathbb{E}[k^2(X, X')])$ (Jalali et al., 2023), which is an estimate of the number of modes. Maximizing the RKE mode count is equivalent to minimizing the following loss

$$\mathbb{E}_{X,X' \overset{\text{iid}}{\sim} P}[k^2(X, X')]. \tag{1}$$

3.2 MAXIMUM MEAN DISCREPANCY AND KERNEL INCEPTION DISTANCE

The (squared) *maximum mean discrepancy* (MMD) (Gretton et al., 2012) between distributions P, Q, which measures the distance between P and Q, can be written as

$$\mathbb{E}[k(X, X')] + \mathbb{E}[k(Y, Y')] - 2\mathbb{E}[k(X, Y)], \tag{2}$$

where $X, X' \overset{\text{iid}}{\sim} P$ and $Y, Y' \overset{\text{iid}}{\sim} Q$, and k is a positive definite kernel. Suppose P is the distribution of samples from a generative model, and Q is a reference distribution. Minimizing the MMD can ensure that P is close to Q. The *Kernel Inception Distance* (KID) (Bińkowski et al., 2018), a popular quality metric for image generative models, is obtained by first passing P and Q through the Inception network (Szegedy et al., 2016), and then computing their MMD, i.e., we have

$$\mathbb{E}[k(\psi(X), \psi(X'))] + \mathbb{E}[k(\psi(Y), \psi(Y'))] - 2\mathbb{E}[k(\psi(X), \psi(Y))], \tag{3}$$

where ψ is the mapping from x to its Inception representation.

4 OPTIMAL MIXTURES OF GENERATIVE MODELS

RKE (1), MMD (2) and KID (3) can all be written as a loss function in the following form

$$L(P) := \mathbb{E}_{X,X' \overset{\text{iid}}{\sim} P}[\kappa(X, X')] + \mathbb{E}_{X \sim P}[f(X)], \tag{4}$$

where $\kappa : \mathcal{X}^2 \to \mathbb{R}$ is a positive semidefinite kernel, and $f : \mathcal{X} \to \mathbb{R}$ is a function. For (1), we take $\kappa(x, x') = k^2(x, x')$ (the square of a kernel is still a kernel) and $f(x) = 0$. For (2), we take $\kappa(x, x') = k(x, x')$ and $f(x) = -2\mathbb{E}_{Y \sim Q}[k(x, Y)]$ (the constant term $\mathbb{E}[k(Y, Y')]$ does not matter). For KID (3), we take $\kappa(x, x') = k(\psi(x), \psi(x'))$ and $f(x) = -2\mathbb{E}_{Y \sim Q}[k(\psi(x), \psi(Y))]$. Note that any convex combinations of (1), (2) and (3) is still in the form (4).

Suppose we are given m generative models, where model i generates samples from the distribution P_i. If our goal is merely to find the model that minimize the loss (4), we should select $\operatorname{argmin}_i L(P_i)$. Nevertheless, for diversity metrics such as RKE, it is possible that a mixture of the models will give a better diversity. Assume that the mixture weight of model i is $\alpha_i \in [0, 1]$, where $\boldsymbol{\alpha} = (\alpha_1, \ldots, \alpha_m)$ is a probability vector. The loss of the mixture distribution $\sum_{i=1}^m \alpha_i P_i$ can then be expressed as

$$L(\boldsymbol{\alpha}) := L\Big(\sum_{i=1}^m \alpha_i P_i\Big) = \boldsymbol{\alpha}^\top \mathbf{K} \boldsymbol{\alpha} + \mathbf{f}^\top \boldsymbol{\alpha},$$

$$\mathbf{K} := (\mathbb{E}_{X \sim P_i,\, X' \sim P_j}[\kappa(X, X')])_{i,j \in [m]} \in \mathbb{R}^{m \times m}, \quad \mathbf{f} := (\mathbb{E}_{X \sim P_i}[f(X)])_{i=1}^m \in \mathbb{R}^m.$$

Given $\mathbf{K}, \mathbf{f}$, the probability vector $\boldsymbol{\alpha}$ minimizing $L(\boldsymbol{\alpha})$ can be found via a convex quadratic program.

In practice, we do not know the precise $\mathbf{K}, \mathbf{f}$, and have to estimate them using samples. Suppose we have the samples $x_{i,1}, \ldots, x_{i,n_i}$ from the distribution P_i for $i = 1, \ldots, m$, where n_i is the number of observed samples from model i. Write $\mathbf{x} := (x_{i,a})_{i \in [m],\, a \in [n_i]}$. We approximate the true mixture distribution $\sum_{i=1}^m \alpha_i P_i$ by the empirical mixture distribution $\sum_{i=1}^m \frac{\alpha_i}{n_i} \sum_{a=1}^{n_i} \delta_{x_{i,a}}$, where we assign a weight α_i / n_i to samples $x_{i,a}$ from model i, and $\delta_{x_{i,a}}$ denotes the degenerate distribution at $x_{i,a}$. We then approximate $L(\boldsymbol{\alpha})$ by the sample loss

$$\hat{L}(\boldsymbol{\alpha}; \mathbf{x}) := L\Big(\sum_{i=1}^m \frac{\alpha_i}{n_i} \sum_{a=1}^{n_i} \delta_{x_{i,a}}\Big) = \boldsymbol{\alpha}^\top \hat{\mathbf{K}}(\mathbf{x}) \boldsymbol{\alpha} + \hat{\mathbf{f}}(\mathbf{x})^\top \boldsymbol{\alpha}, \tag{5}$$

[2] The order-2 Rényi entropy for discrete distributions is a special case by taking $k(x, x') = \mathbf{1}_{x = x'}$.

$$\hat{\mathbf{K}}(\mathbf{x}) := \Big(\frac{1}{n_i n_j}\sum_{a=1}^{n_i}\sum_{b=1}^{n_j}\kappa(x_{i,a}, x_{j,b})\Big)_{i,j} \in \mathbb{R}^{m\times m}, \quad \hat{\mathbf{f}}(\mathbf{x}) := \Big(\frac{1}{n_i}\sum_{a=1}^{n_i} f(x_{i,a})\Big)_{i=1}^{m} \in \mathbb{R}^m.$$

The minimization of $\hat{L}(\boldsymbol{\alpha}; \mathbf{x})$ over probability vectors $\boldsymbol{\alpha}$ is still a convex quadratic program.

5 Online Selection of Optimal Mixtures – Mixture Multi-Armed Bandit

Suppose we are given m generative models, but we do not have any prior information about them. Our goal is to use these models to generate a collection of samples $(x^{(t)})_{i\in[T]}$ in T rounds that minimizes the loss (4) $L(\hat{P}^{(T)})$ at the empirical distribution $\hat{P}^{(T)} = T^{-1}\sum_{t=1}^{T}\delta_{x^{(t)}}$. We have

$$L(\hat{P}^{(T)}) = \frac{1}{T^2}\sum_{s,t\in[T]}\kappa(x^{(s)}, x^{(t)}) + \frac{1}{T}\sum_{t=1}^{T} f(x^{(t)}).$$

If we are told by an oracle the optimal mixture $\boldsymbol{\alpha}^*$ that minimizes the loss $L(\boldsymbol{\alpha})$, then we should generate samples according to this mixture distribution, giving $\approx \alpha_i^* T$ samples from model i. We call this the *mixture oracle* scenario. Nevertheless, in reality, we do not know $\mathbf{K}, \mathbf{f}$, and cannot compute $\boldsymbol{\alpha}^*$ exactly. Instead, we have to approximate $\boldsymbol{\alpha}^*$ by minimizing the sample loss $\hat{L}(\boldsymbol{\alpha}; \mathbf{x})$ (5). However, we do not have the samples $\mathbf{x}$ at the beginning in order to compute $\hat{L}(\boldsymbol{\alpha}; \mathbf{x})$, so we have to generate some samples first. Yet, to generate these initial samples, we need an estimate of $\boldsymbol{\alpha}^*$, or else those samples may have a suboptimal empirical distribution and affect our final loss $L(\hat{P}^{(T)})$, or we will have to discard those initial samples which results in wastage.

This "chicken and egg" problem is naturally solved by an online learning approach via multi-armed bandit. At time $t = 1, \dots, T$, we choose and pull an arm $b^{(t)} \in [m]$ (i.e., generate a sample from model $b^{(t)}$), and obtain a sample $x^{(t)}$ from the distribution $P_{b^{(t)}}$. The choice $b^{(t)}$ can depend on all previous samples $x^{(1)}, \dots, x^{(t-1)}$. Unlike conventional multi-armed bandit where the goal is to maximize the total reward over T rounds, here we minimize the loss $L(\hat{P}^{(T)})$ which involve cross terms $\kappa(x^{(s)}, x^{(t)})$ between samples at different rounds. Note that if $\kappa(x, x') = 0$, then this reduces to the conventional multi-armed bandit setting by taking $f(x)$ to be the negative reward of the sample x. In the following subsections, we will propose two new algorithms that are generalizations of the upper confidence bound (UCB) algorithm for multi-armed bandit (Agrawal, 1995a; Auer, 2003).

5.1 Mixture Upper Confidence Bound – Continuum-Armed Bandit

Let $n_i^{(t)}$ be the number of times arm i has been pulled up to time t. Let $\mathbf{x}^{(t)} := (x_{i,a})_{i\in[m],\, a\in[n_i^{(t)}]}$ be the observed samples up to time t. We focus on bounded loss functions, and assume that $\kappa : \mathcal{X}^2 \to [\kappa_0, \kappa_1]$ and $f : \mathcal{X} \to [f_0, f_1]$ are bounded. Let $\Delta_\kappa := \kappa_1 - \kappa_0$, $\Delta_f := f_1 - f_0$. Define the *sensitivity* of L as $\Delta_L := 2\Delta_\kappa + \Delta_f$.

We now present the *mixture upper confidence bound – continuum-armed bandit (Mixture-UCB-CAB) algorithm*. It has a parameter $\beta > 1$. It treats the online selection problem as multi-armed bandit with infinitely many arms similar to the continuum-armed bandit settings in (Agrawal, 1995b; Lu et al., 2019). Each arm is a probability vector $\boldsymbol{\alpha}$. By pulling the arm $\boldsymbol{\alpha}$, we generate a sample from a randomly chosen model, where model i is chosen with probability α_i. Refer to Algorithm 1. Similar to UCB, Mixture-UCB-CAB finds a lower confidence bound $\hat{L}(\boldsymbol{\alpha}; \mathbf{x}^{(t)}) - (\boldsymbol{\epsilon}^{(t)})^\top \boldsymbol{\alpha}$ of the true loss $L(\boldsymbol{\alpha})$ at each round. To justify the expressions (6), (7), we prove that $\hat{L}(\boldsymbol{\alpha}; \mathbf{x}^{(t)}) - (\boldsymbol{\epsilon}^{(t)})^\top \boldsymbol{\alpha}$ in (6) lower-bounds $L(\boldsymbol{\alpha})$ with probability at least $1 - t^{-\beta}$. The proof is given in Appendix 8.1.

Theorem 1 *Fix a probability vector $\boldsymbol{\alpha}$.*[4] *Suppose we have samples $x_{i,1}, \dots, x_{i,n_i}$ from the distribution P_i for $i = 1, \dots, m$, where n_i is the number of observed samples from model i. For $\delta > 0$,*

$$\mathbb{P}\big(\hat{L}(\boldsymbol{\alpha}; \mathbf{x}) - L(\boldsymbol{\alpha}) \ge \boldsymbol{\epsilon}(\delta)^\top \boldsymbol{\alpha}\big) \le \delta, \quad \mathbb{P}\big(L(\boldsymbol{\alpha}) - \hat{L}(\boldsymbol{\alpha}; \mathbf{x}) \ge \boldsymbol{\epsilon}(\delta)^\top \boldsymbol{\alpha}\big) \le \delta,$$

[4] Theorem 1 holds for a fixed $\boldsymbol{\alpha}$. A worst-case bound that simultaneously holds for every $\boldsymbol{\alpha}$ is in Lemma 1.

Algorithm 1 Mixture-UCB-CAB

Input: m generative arms, number of rounds T
Output: Gathered samples $\mathbf{x}^{(T)}$
for $t \in \{0, \dots, m-1\}$ **do**
  Pull arm $t+1$ at time $t+1$ to obtain sample $x_{t+1,1} \sim P_{t+1}$. Set $n_{t+1}^{(m)} = 1$.
end for
for $t \in \{m, \dots, T-1\}$ **do**
  Compute an estimate of the optimal mixture distribution via the convex quadratic program:

$$\boldsymbol{\alpha}^{(t)} := \operatorname{argmin}_{\boldsymbol{\alpha}} \big(\hat{L}(\boldsymbol{\alpha}; \mathbf{x}^{(t)}) - (\boldsymbol{\epsilon}^{(t)})^\top \boldsymbol{\alpha} \big), \tag{6}$$

  where the minimization is over probability vectors $\boldsymbol{\alpha}$, and $\boldsymbol{\epsilon}^{(t)} \in \mathbb{R}^m$ is defined as

$$\epsilon_i^{(t)} := \Delta_L \sqrt{(\beta \log t)/(2n_i^{(t)})} + \Delta_\kappa / n_i^{(t)}. \tag{7}$$

  Generate the arm index $b^{(t+1)} \in [m]$ at random with $\mathbb{P}(b^{(t+1)} = i) = \alpha_i^{(t)}$.
  Pull arm $b = b^{(t+1)}$ at time $t+1$ to obtain a new sample $x_{b, n_b^{(t)}+1} \sim P_b$. Set $n_b^{(t+1)} = n_b^{(t)} + 1$ and $n_j^{(t+1)} = n_j^{(t)}$ for $j \neq b$.[3]
end for
return samples $\mathbf{x}^{(T)}$

where $\boldsymbol{\epsilon}(\delta) := \big(\Delta_L \sqrt{\frac{\log(1/\delta)}{2n_i}} + \frac{\Delta_\kappa}{n_i} \big)_{i \in [m]}$.

We now prove that Mixture-UCB-CAB gives an expected loss $\mathbb{E}[L(\hat{P}^{(T)})]$ that converges to the optimal loss $\min_{\boldsymbol{\alpha}} L(\boldsymbol{\alpha})$ by bounding their gap. This means that Mixture-UCB-CAB is a zero-regret strategy by treating $\mathbb{E}[L(\hat{P}^{(T)})] - \min_{\boldsymbol{\alpha}} L(\boldsymbol{\alpha})$ as the average regret per round.[5] The proof is given in Appendix 8.4.

Theorem 2 *Suppose $m \geq 2$, $\beta \geq 4$. Consider bounded quadratic loss function (4) with κ being positive semidefinite. Let $\hat{P}^{(T)}$ be the empirical distribution of the first $T \geq 2$ samples $\mathbf{x}^{(T)}$ given by Mixture-UCB-CAB. Then the gap between the expected loss and the optimal loss is bounded by*

$$\mathbb{E}\big[L(\hat{P}^{(T)})\big] - \min_{\boldsymbol{\alpha}} L(\boldsymbol{\alpha}) \leq 4\Delta_L \sqrt{\frac{\beta m \log T}{T}}.$$

When $\kappa(x, x') = 0$, Mixture-UCB-CAB reduces to the conventional UCB, and Theorem 2 coincides with the $O(\sqrt{(m \log T)/T})$ distribution-free bound on the regret per round of conventional UCB (Bubeck & Cesa-Bianchi, 2012). Since there is a $\Omega(\sqrt{m/T})$ minimax lower bound on the regret per round even for conventional multi-armed bandit without the quadratic kernel term (Bubeck & Cesa-Bianchi, 2012, Theorem 3.4), Theorem 2 is tight up to a logarithmic factor.

The main difference between Mixture-UCB-CAB and conventional UCB is that we choose a mixture of arms in (6) given by the probability vector $\boldsymbol{\alpha}$, instead of a single arm. A more straightforward application of UCB would be to simply find the single arm that minimizes the lower bound in (6), i.e., we restrict $\boldsymbol{\alpha} = \mathbf{e}_i$ for some $i \in [m]$, where $\mathbf{e}_i$ is the i-th basis vector, and minimize (6) over i instead. We call this *Vanilla-UCB*. Vanilla-UCB fails to take into account the possibility that a mixture may give a smaller loss than every single arm. In the long run, Vanilla-UCB converges to pulling the best single arm instead of the optimal mixture. Vanilla-UCB will be used as a baseline to be compared with Mixture-UCB-CAB, and another new algorithm presented in the next section.

[5] To justify calling $R := \mathbb{E}[L(\hat{P}^{(T)})] - \min_{\boldsymbol{\alpha}} L(\boldsymbol{\alpha})$ the average regret per round, note that when $\kappa(x, x') = 0$ and $f(x) = -r(x)$ where $r(x)$ is the reward of the sample x, i.e., the loss $L(P) = \mathbb{E}_{X \sim P}[f(X)]$ is linear, $T(\mathbb{E}[L(\hat{P}^{(T)})] - \min_{\boldsymbol{\alpha}} L(\boldsymbol{\alpha})) = T \max_{i \in [m]} \mathbb{E}_{X \sim P_i}[r(X)] - \mathbb{E}[\sum_{t=1}^T r(x^{(t)})]$ indeed reduces to the conventional notion of regret. So R can be regarded as the quadratic generalization of regret.

Algorithm 2 Mixture-UCB-OGD

1: **Input:** m generative arms, number of rounds T
2: **Output:** Gathered samples $\mathbf{x}^{(T)}$
3: **for** $t \in \{0, \ldots, m-1\}$ **do**
4: Pull arm $t+1$ at time $t+1$ to obtain sample $x_{t+1,1} \sim P_{t+1}$
5: **end for**
6: **for** $t \in \{m, \ldots, T-1\}$ **do**
7: Compute the gradient

$$\mathbf{h}^{(t)} := \nabla_{\boldsymbol{\alpha}} \left(\hat{L}(\boldsymbol{\alpha}; \mathbf{x}^{(t)}) - (\boldsymbol{\epsilon}^{(t)})^\top \boldsymbol{\alpha} \right) \Big|_{\boldsymbol{\alpha}=\mathbf{n}^{(t)}/t} = \frac{2}{t} \hat{\mathbf{K}}(\mathbf{x}^{(t)}) \mathbf{n}^{(t)} + \hat{\mathbf{f}}(\mathbf{x}^{(t)}) - \boldsymbol{\epsilon}^{(t)}, \quad (8)$$

where $\mathbf{n}^{(t)} := (n_i^{(t)})_{i \in [m]} \in \mathbb{R}^m$, and $\boldsymbol{\epsilon}^{(t)}$ is defined as in Mixture-UCB-CAB
8: Pull arm $b = b^{(t+1)} := \operatorname{argmin}_i h_i^{(t)}$ at time $t+1$ to obtain a new sample $x_{b,n_b^{(t)}+1} \sim P_b$.
9: **end for**
10: **return** samples $\mathbf{x}^{(T)}$

Mixture-UCB-CAB can be extended to the Sparse-Mixture-UCB-CAB algorithm which eventually select only a small number of models. This can be useful if there is a subscription cost for each model. Refer to Appendix 8.2 for discussions.

5.2 Mixture Upper Confidence Bound – Online Gradient Descent

We present an alternative to Mixture-UCB-CAB, called the *mixture upper confidence bound – online gradient descent (Mixture-UCB-OGD) algorithm*, inspired by the online gradient descent algorithm (Shalev-Shwartz et al., 2012). It also has a parameter $\beta > 1$. Refer to Algorithm 2.
Mixture-UCB-CAB and Mixture-UCB-OGD can both be regarded as generalizations of the original UCB algorithm, in the sense that they reduce to UCB when $\kappa(x, x') = 0$. If we remove the $\frac{2}{t}\hat{\mathbf{K}}(\mathbf{x})\mathbf{n}^{(t)}$ term in (8), then Mixture-UCB-OGD becomes the same as UCB.

Both Mixture-UCB-CAB and Mixture-UCB-OGD attempt to make the "proportion vector" $\mathbf{n}^{(t)}/t$ (note that $n_i^{(t)}/t$ is the proportion of samples from model i) approach the optimal mixture $\boldsymbol{\alpha}^*$ that minimizes $\hat{L}(\boldsymbol{\alpha})$, but they do so in different manners. Mixture-UCB-CAB first computes the estimate $\boldsymbol{\alpha}^{(t)}$ after time t, then approaches $\boldsymbol{\alpha}^{(t)}$ by pulling an arm randomly chosen from the distribution $\boldsymbol{\alpha}^{(t)}$. Mixture-UCB-OGD estimates the gradient $\mathbf{h}^{(t)}$ of the loss function at the current proportion vector $\mathbf{n}^{(t)}/t$, and pulls an arm that results in the steepest descent of the loss.

An advantage of Mixture-UCB-OGD is that the computation of gradient (8) is significantly faster than the quadratic program (6) in Mixture-UCB-CAB. The running time complexity of Mixture-UCB-OGD is $O(T^2 + Tm^2)$.[6] Nevertheless, a regret bound for Mixture-UCB-OGD similar to Theorem 2 seems to be difficult to derive, and is left for future research.

6 Numerical Results

We experiment on various scenarios to showcase the performance of our proposed algorithms. The experiments involve the following algorithms:

- **Mixture Oracle.** In the mixture oracle algorithm (Section 5), an oracle tells us the optimal mixture $\boldsymbol{\alpha}^*$ in advance, and we pull arms randomly according to this distribution. The optimal mixture is calculated by solving the quadratic optimization in Section 4 on a large number of samples for

[5] We may also consider the scenario where each pull gives a batch of l samples instead of only one sample. In this case, we will have $x_{b,n_b^{(t-1)}+1}, \ldots, x_{b,n_b^{(t-1)}+l} \sim P_b$ and $n_b^{(t)} = n_b^{(t-1)} + l$.

[6] To update $\hat{\mathbf{K}}(\mathbf{x}^{(t)})$ after a new sample x' is obtained, we only need to compute $\kappa(x, x')$ for each existing sample x, and add their contributions to the corresponding entries in $\hat{\mathbf{K}}(\mathbf{x}^{(t)})$, requiring a computational time that is linear with the number of existing samples.

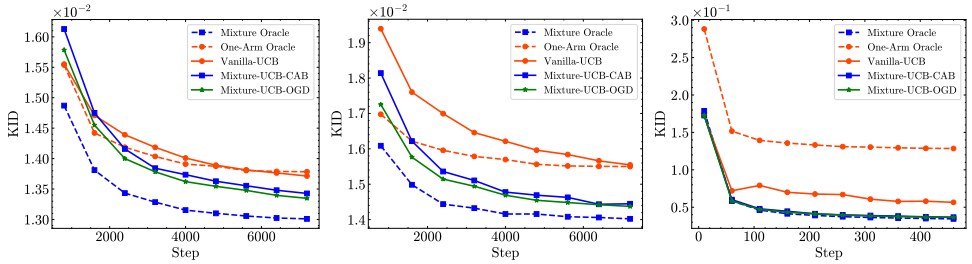

(a) FFHQ generators (b) LSUN-Bedroom generators (c) FFHQ truncated generators

Figure 2: Performance comparison of online algorithms for the KID metric across FFHQ, LSUN-Bedroom, and FFHQ Truncated generators.

each arm. The number of chosen samples varies based on the experiments. This is an unrealistic setting that only serves as a theoretical upper bound of the performance of any online algorithm. A realistic algorithm that performs close to the mixture oracle would be almost optimal.

- **One-Arm Oracle.** An oracle tells us the optimal single arm in advance, and we keep pulling this arm. This is an unrealistic setting. If our algorithms outperform the one-arm oracle, this will show that the advantage of pulling a mixture of arms (instead of a single arm) can be realistically achieved via online algorithms.
- **Vanilla-UCB.** A direct application of UCB mentioned near the end of Section 5.1. This serves as a baseline for the purpose of comparison.
- **Mixture-UCB-CAB.** The mixture upper confidence bound – continuum-armed bandit algorithm proposed in Section 5.1.
- **Mixture-UCB-OGD.** The mixture upper confidence bound – online gradient descent algorithm proposed in Section 5.2.

Experiments Setup. We used DINOv2-ViT-L/14 (Oquab et al., 2024) for image feature extraction, as recommended in (Stein et al., 2023), and utilized RoBERTa (Liu et al., 2019) as the text encoder. Detailed explanation of the setup for each experiment is presented in Section 8.3.

6.1 Optimal Mixture for Diversity and Quality via KID

We conducted three experiments to evaluate our method using the Kernel Inception Distance (KID) metric. In the first experiment, we used five distinct generative models: LDM (Rombach et al., 2022), StyleGAN-XL (Sauer et al., 2022), Efficient-vdVAE (Hazami et al., 2022), InsGen (Yang et al., 2021), and StyleNAT (Walton et al., 2023), all trained on the FFHQ dataset (Karras et al., 2019b). In the second experiment, we used generated images from four models[7]: StyleGAN (Karras et al., 2019a), Projected GAN (Sauer et al., 2021b), iDDPM (Nichol & Dhariwal, 2021), and Unleashing Transformers (Bond-Taylor et al., 2021), all trained on the LSUN-Bedroom dataset (Yu et al., 2016). This experiment followed a similar setup to the first. In the final experiment, we employed the truncation method (Marchesi, 2017; Karras et al., 2019b) to generate diversity-controlled images centered on eight randomly selected points, using StyleGAN2-ADA (Karras et al., 2020), also trained on the FFHQ dataset. Figure 2 demonstrates that the mixture of generators achieves better KID scores compared to individual models. Additionally, the two Mixture-UCB algorithms consistently outperform the baselines.

6.2 Optimal Mixture for Diversity via RKE

We used the RKE Mode Count (Jalali et al., 2023) as an evaluation metric to show the effect of mixing the models on the diversity and the advantage of our algorithms Mixture-UCB-CAB and Mixture-UCB-OGD. The score in the plots is the RKE Mode Count, written as RKE for brevity.

[7]FFHQ and LSUN-Bedroom datasets were downloaded from the dgm-eval repository (Stein et al., 2023) (licensed under MIT license): https://github.com/layer6ai-labs/dgm-eval.

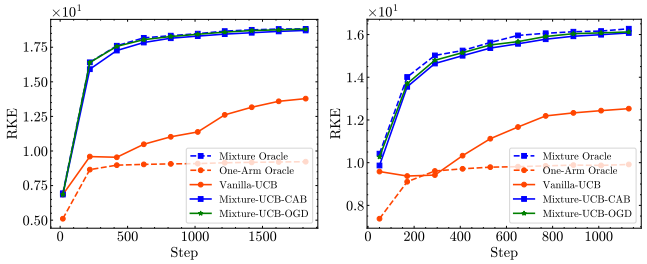

(a) FFHQ truncated generators (b) AFHQ truncated generators

Figure 3: Performance comparison of online algorithms based on the RKE metric for Simulator Unconditional Generative Models.

Synthetic Unconditional Generative Models We conduct two experiments on diversity-limited generative models. First, we used eight center points with a truncation value of 0.3 to generate images using StyleGAN2-ADA, trained on the FFHQ dataset. In the second experiment, we applied the same model, trained on the AFHQ Cat dataset (Choi et al., 2020), with a truncation value of 0.4. As shown in Figure 3, the mixture achieves a higher RKE score, and our algorithms consistently give a higher RKE value throughout the sampling rounds. The increase in diversity is visually depicted in Figures 7 and 8.

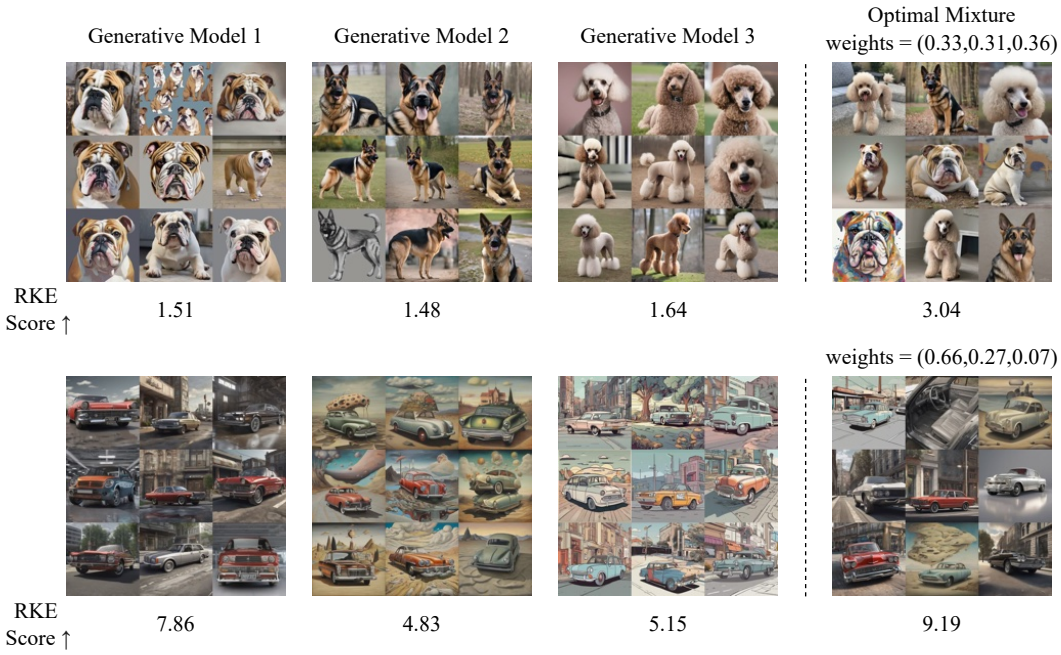

Figure 4: Visual comparison of the diversity across individual arms and the optimal mixture for Dog Breed Generators and Style-Specific Generators.

Text to Image Generative Models We used Stable Diffusion XL (Podell et al., 2023) with specific prompts to create three car image generators with distinct styles: realistic, surreal, and cartoon. In the second experiment, recognizing the importance of diversity in generative models for design tasks, we used five models—FLUX.1-Schnell (Lab, 2024), Kandinsky 3.0 (Arkhipkin et al., 2024), PixArt-α (Chen et al., 2023a), and Stable Diffusion XL—to generate images of the object "Sofa". In a similar manner, we generated green giraffe images using Kandinsky 3.0, Stable Diffusion 3 (Esser et al., 2024), and PixArt-α, as shown in Figure 1.. Finally, in the third experiment, we used Stable Diffusion XL to simulate models generating images of different dog breeds: Bulldog, German Shepherd, and Poodle, respectively. This illustrates the challenge of generating diverse object types with text-to-image models. Figure 4 illustrates the impact of using a mixture of models in the first and third experiments. The improvement in diversity is evident both visually and quantitatively, as

reflected in the RKE Scores. As shown in Figure 5, our online algorithms consistently outperform others in generating more diverse samples.

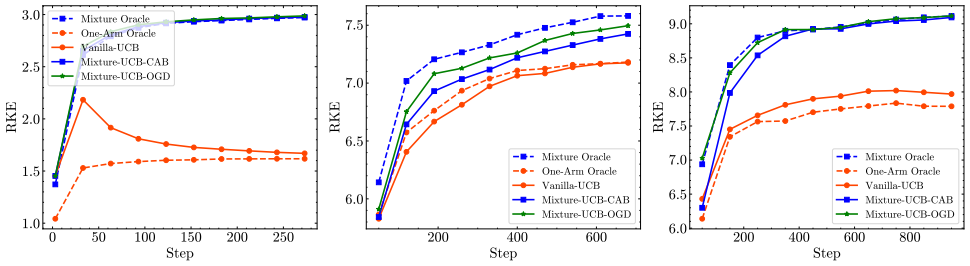

(a) Dog breed generators (b) Sofa image generators (c) Style-specific generators

Figure 5: Performance comparison of online algorithms using the RKE metric for text-to-image generative models.

Text Generative Models We utilized the OpenLLMText dataset (Chen et al., 2023b), which comprises 60,000 human texts rephrased paragraph by paragraph using the GPT2-XL (Radford et al., 2019), LLaMA-7B (Touvron et al., 2023), and PaLM (Chowdhery et al., 2022) models. To extract textual features, we employed the RoBERTa Text Encoder. As shown in Figure 11a in Section 8.3.2, the results demonstrate the advantage of our online algorithms, suggesting that our method applies not only to image generators but also to text generators.

6.3 Optimal Mixture for Diversity and Quality via RKE and Precision/Density

Using RKE, we focus solely on the diversity of the arms without accounting for their quality. To address this, we apply our methodology to both RKE and Precision (Kynkäänniemi et al., 2019), as well as RKE and Density (Naeem et al., 2020). We conduct experiments in which quality is a key consideration. We use four arms: three are StyleGAN2-ADA models trained on the FFHQ dataset, each generating images with a truncation of 0.3 around randomly selected center points. The fourth model is StyleGAN2-ADA trained on CIFAR-10 (Krizhevsky & Hinton, 2009). The FFHQ dataset is used as the reference dataset. Figures 6 and 12 demonstrate the ability of our algorithms in finding optimal mixtures with higher diversity/quality score.

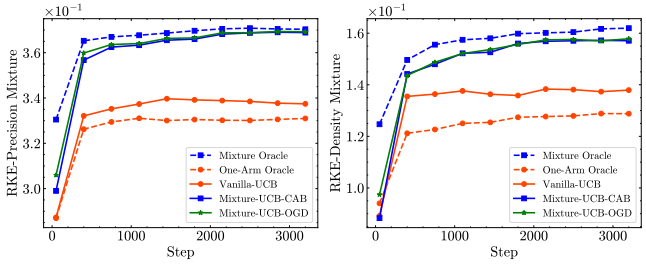

(a) RKE w/Precision (b) RKE w/Density

Figure 6: Performance comparison of online algorithms using the combination of RKE with Precision and RKE with Density metrics.

7 Conclusion

We studied the online selection from several generative models, where the online learner aims to generate samples with the best overall quality and diversity. While standard multi-armed bandit (MAB) algorithms aim to converge to one arm and select one generative model, we highlighted the fact that a mixture of generative models could achieve a higher score compared to each individual model. We proposed the Mixture-UCB-CAB and Mixture-UCB-OGD online learning algorithms to find the optimal mixture. Our experiments suggest the usefulness of the algorithm in improving the performance scores over individual arms. Extending the algorithm to conditional and text-based generative models is a topic for future exploration. In addition, the application of the algorithm to other data domains, including text, audio, and video, is an interesting future direction.

REFERENCES

Rajeev Agrawal. Sample mean based index policies by $O(\log n)$ regret for the multi-armed bandit problem. *Advances in applied probability*, 27(4):1054–1078, 1995a.

Rajeev Agrawal. The continuum-armed bandit problem. *SIAM Journal on Control and Optimization*, 33(6):1926–1951, 1995b. doi: 10.1137/S0363012992237273. URL https://doi.org/10.1137/S0363012992237273.

Martin Arjovsky, Soumith Chintala, and Léon Bottou. Wasserstein generative adversarial networks. In Doina Precup and Yee Whye Teh (eds.), *Proceedings of the 34th International Conference on Machine Learning*, volume 70 of *Proceedings of Machine Learning Research*, pp. 214–223. PMLR, 06–11 Aug 2017. URL https://proceedings.mlr.press/v70/arjovsky17a.html.

Vladimir Arkhipkin, Andrei Filatov, Viacheslav Vasilev, Anastasia Maltseva, Said Azizov, Igor Pavlov, Julia Agafonova, Andrey Kuznetsov, and Denis Dimitrov. Kandinsky 3.0 technical report, 2023.

Vladimir Arkhipkin, Andrei Filatov, Viacheslav Vasilev, Anastasia Maltseva, Said Azizov, Igor Pavlov, Julia Agafonova, Andrey Kuznetsov, and Denis Dimitrov. Kandinsky 3.0 technical report, 2024. URL https://arxiv.org/abs/2312.03511.

Peter Auer. Using confidence bounds for exploitation-exploration trade-offs. *J. Mach. Learn. Res.*, 3:397–422, March 2003. ISSN 1532-4435.

Mikołaj Bińkowski, Danica J Sutherland, Michael Arbel, and Arthur Gretton. Demystifying MMD GANs. In *International Conference on Learning Representations*, 2018.

Sam Bond-Taylor, Peter Hessey, Hiroshi Sasaki, Toby P. Breckon, and Chris G. Willcocks. Unleashing transformers: Parallel token prediction with discrete absorbing diffusion for fast high-resolution image generation from vector-quantized codes, 2021. URL https://arxiv.org/abs/2111.12701.

Sébastien Bubeck, Gilles Stoltz, Csaba Szepesvári, and Rémi Munos. Online optimization in x-armed bandits. In D. Koller, D. Schuurmans, Y. Bengio, and L. Bottou (eds.), *Advances in Neural Information Processing Systems*, volume 21. Curran Associates, Inc., 2008. URL https://proceedings.neurips.cc/paper_files/paper/2008/file/f387624df552cea2f369918c5e1e12bc-Paper.pdf.

Sébastien Bubeck and Nicolò Cesa-Bianchi. Regret analysis of stochastic and nonstochastic multi-armed bandit problems, 2012. URL https://arxiv.org/abs/1204.5721.

Junsong Chen, Jincheng Yu, Chongjian Ge, Lewei Yao, Enze Xie, Yue Wu, Zhongdao Wang, James Kwok, Ping Luo, Huchuan Lu, and Zhenguo Li. Pixart-α: Fast training of diffusion transformer for photorealistic text-to-image synthesis, 2023a. URL https://arxiv.org/abs/2310.00426.

Luming Chen and Sujit K Ghosh. Fast model selection and hyperparameter tuning for generative models. *Entropy*, 26(2):150, 2024.

Yutian Chen, Hao Kang, Yiyan Zhai, Liangze Li, Rita Singh, and Bhiksha Raj. Openllmtext dataset, 2023b. URL https://zenodo.org/doi/10.5281/zenodo.8285326.

Yunjey Choi, Youngjung Uh, Jaejun Yoo, and Jung-Woo Ha. Stargan v2: Diverse image synthesis for multiple domains, 2020. URL https://arxiv.org/abs/1912.01865.

Aakanksha Chowdhery, Sharan Narang, Jacob Devlin, Maarten Bosma, Gaurav Mishra, Adam Roberts, Paul Barham, Hyung Won Chung, Charles Sutton, Sebastian Gehrmann, Parker Schuh, Kensen Shi, Sasha Tsvyashchenko, Joshua Maynez, Abhishek Rao, Parker Barnes, Yi Tay, Noam Shazeer, Vinodkumar Prabhakaran, Emily Reif, Nan Du, Ben Hutchinson, Reiner Pope, James Bradbury, Jacob Austin, Michael Isard, Guy Gur-Ari, Pengcheng Yin, Toju Duke, Anselm Levskaya, Sanjay Ghemawat, Sunipa Dev, Henryk Michalewski, Xavier Garcia, Vedant Misra, Kevin

Robinson, Liam Fedus, Denny Zhou, Daphne Ippolito, David Luan, Hyeontaek Lim, Barret Zoph, Alexander Spiridonov, Ryan Sepassi, David Dohan, Shivani Agrawal, Mark Omernick, Andrew M. Dai, Thanumalayan Sankaranarayana Pillai, Marie Pellat, Aitor Lewkowycz, Erica Moreira, Rewon Child, Oleksandr Polozov, Katherine Lee, Zongwei Zhou, Xuezhi Wang, Brennan Saeta, Mark Diaz, Orhan Firat, Michele Catasta, Jason Wei, Kathy Meier-Hellstern, Douglas Eck, Jeff Dean, Slav Petrov, and Noah Fiedel. Palm: Scaling language modeling with pathways, 2022. URL https://arxiv.org/abs/2204.02311.

M. A. Efroymson. Multiple regression analysis. In A. Ralston and H. S. Wilf (eds.), *Mathematical Methods for Digital Computers*, volume 1, pp. 191–203. John Wiley & Sons, Inc., 1960.

Patrick Esser, Sumith Kulal, Andreas Blattmann, Rahim Entezari, Jonas Müller, Harry Saini, Yam Levi, Dominik Lorenz, Axel Sauer, Frederic Boesel, Dustin Podell, Tim Dockhorn, Zion English, Kyle Lacey, Alex Goodwin, Yannik Marek, and Robin Rombach. Scaling rectified flow transformers for high-resolution image synthesis, 2024. URL https://arxiv.org/abs/2403.03206.

Matthias Feurer and Frank Hutter. *Hyperparameter Optimization*, pp. 3–33. Springer International Publishing, Cham, 2019. ISBN 978-3-030-05318-5. doi: 10.1007/978-3-030-05318-5_1. URL https://doi.org/10.1007/978-3-030-05318-5_1.

Dan Friedman and Adji Bousso Dieng. The vendi score: A diversity evaluation metric for machine learning, 2023. URL https://arxiv.org/abs/2210.02410.

Arthur Gretton, Karsten M Borgwardt, Malte J Rasch, Bernhard Schölkopf, and Alexander Smola. A kernel two-sample test. *The Journal of Machine Learning Research*, 13(1):723–773, 2012.

Louay Hazami, Rayhane Mama, and Ragavan Thurairatnam. Efficient-vdvae: Less is more, 2022. URL https://arxiv.org/abs/2203.13751.

Martin Heusel, Hubert Ramsauer, Thomas Unterthiner, Bernhard Nessler, and Sepp Hochreiter. Gans trained by a two time-scale update rule converge to a local nash equilibrium, 2018. URL https://arxiv.org/abs/1706.08500.

Xiaoyan Hu, Ho fung Leung, and Farzan Farnia. An optimism-based approach to online evaluation of generative models, 2024. URL https://arxiv.org/abs/2406.07451.

Mohammad Jalali, Cheuk Ting Li, and Farzan Farnia. An information-theoretic evaluation of generative models in learning multi-modal distributions. *Advances in Neural Information Processing Systems*, 36, 2023.

Kevin Jamieson and Ameet Talwalkar. Non-stochastic best arm identification and hyperparameter optimization. In *Artificial intelligence and statistics*, pp. 240–248. PMLR, 2016.

Zohar Karnin, Tomer Koren, and Oren Somekh. Almost optimal exploration in multi-armed bandits. In *International conference on machine learning*, pp. 1238–1246. PMLR, 2013.

Tero Karras, Samuli Laine, and Timo Aila. A style-based generator architecture for generative adversarial networks. In *2019 IEEE/CVF Conference on Computer Vision and Pattern Recognition (CVPR)*, pp. 4396–4405, 2019a. doi: 10.1109/CVPR.2019.00453.

Tero Karras, Samuli Laine, and Timo Aila. A style-based generator architecture for generative adversarial networks, 2019b. URL https://arxiv.org/abs/1812.04948.

Tero Karras, Miika Aittala, Janne Hellsten, Samuli Laine, Jaakko Lehtinen, and Timo Aila. Training generative adversarial networks with limited data, 2020. URL https://arxiv.org/abs/2006.06676.

Robert Kleinberg. Nearly tight bounds for the continuum-armed bandit problem. In *Proceedings of the 17th International Conference on Neural Information Processing Systems*, NIPS'04, pp. 697–704, Cambridge, MA, USA, 2004. MIT Press.

Robert Kleinberg, Aleksandrs Slivkins, and Eli Upfal. Bandits and experts in metric spaces, 2019. URL https://arxiv.org/abs/1312.1277.

Alex Krizhevsky and Geoffrey Hinton. Learning multiple layers of features from tiny images. Technical Report 0, University of Toronto, Toronto, Ontario, 2009. URL https://www.cs.toronto.edu/~kriz/learning-features-2009-TR.pdf.

Tuomas Kynkäänniemi, Tero Karras, Samuli Laine, Jaakko Lehtinen, and Timo Aila. Improved precision and recall metric for assessing generative models, 2019. URL https://arxiv.org/abs/1904.06991.

Black Forest Lab. Flux: A diffusion-based text-to-image (t2i) model. https://github.com/blackforestlab/flux, 2024. Accessed: 2024-09.

T.L Lai and Herbert Robbins. Asymptotically efficient adaptive allocation rules. *Advances in Applied Mathematics*, 6(1):4–22, 1985. ISSN 0196-8858. doi: https://doi.org/10.1016/0196-8858(85)90002-8. URL https://www.sciencedirect.com/science/article/pii/0196885885900028.

Lisha Li, Kevin Jamieson, Giulia DeSalvo, Afshin Rostamizadeh, and Ameet Talwalkar. Hyperband: A novel bandit-based approach to hyperparameter optimization. *Journal of Machine Learning Research*, 18(185):1–52, 2018. URL http://jmlr.org/papers/v18/16-558.html.

Yinhan Liu, Myle Ott, Naman Goyal, Jingfei Du, Mandar Joshi, Danqi Chen, Omer Levy, Mike Lewis, Luke Zettlemoyer, and Veselin Stoyanov. Roberta: A robustly optimized bert pretraining approach, 2019. URL https://arxiv.org/abs/1907.11692.

Shiyin Lu, Guanghui Wang, Yao Hu, and Lijun Zhang. Optimal algorithms for lipschitz bandits with heavy-tailed rewards. In *International Conference on Machine Learning*, pp. 4154–4163. PMLR, 2019.

Marco Marchesi. Megapixel size image creation using generative adversarial networks, 2017. URL https://arxiv.org/abs/1706.00082.

Muhammad Ferjad Naeem, Seong Joon Oh, Youngjung Uh, Yunjey Choi, and Jaejun Yoo. Reliable fidelity and diversity metrics for generative models, 2020. URL https://arxiv.org/abs/2002.09797.

Alex Nichol and Prafulla Dhariwal. Improved denoising diffusion probabilistic models, 2021. URL https://arxiv.org/abs/2102.09672.

OpenAI. Gpt-4 technical overview. https://openai.com/research/gpt-4, 2024. Accessed: 2024-10.

Maxime Oquab, Timothée Darcet, Théo Moutakanni, Huy Vo, Marc Szafraniec, Vasil Khalidov, Pierre Fernandez, Daniel Haziza, Francisco Massa, Alaaeldin El-Nouby, Mahmoud Assran, Nicolas Ballas, Wojciech Galuba, Russell Howes, Po-Yao Huang, Shang-Wen Li, Ishan Misra, Michael Rabbat, Vasu Sharma, Gabriel Synnaeve, Hu Xu, Hervé Jegou, Julien Mairal, Patrick Labatut, Armand Joulin, and Piotr Bojanowski. Dinov2: Learning robust visual features without supervision, 2024. URL https://arxiv.org/abs/2304.07193.

Dustin Podell, Zion English, Kyle Lacey, Andreas Blattmann, Tim Dockhorn, Jonas Müller, Joe Penna, and Robin Rombach. Sdxl: Improving latent diffusion models for high-resolution image synthesis, 2023. URL https://arxiv.org/abs/2307.01952.

Alec Radford, Jeff Wu, Rewon Child, David Luan, Dario Amodei, and Ilya Sutskever. Language models are unsupervised multitask learners. 2019.

Robin Rombach, Andreas Blattmann, Dominik Lorenz, Patrick Esser, and Björn Ommer. High-resolution image synthesis with latent diffusion models, 2022. URL https://arxiv.org/abs/2112.10752.

Mehdi SM Sajjadi, Olivier Bachem, Mario Lucic, Olivier Bousquet, and Sylvain Gelly. Assessing generative models via precision and recall. *Advances in neural information processing systems*, 31, 2018.

Axel Sauer, Kashyap Chitta, Jens Müller, and Andreas Geiger. Projected gans converge faster. In M. Ranzato, A. Beygelzimer, Y. Dauphin, P.S. Liang, and J. Wortman Vaughan (eds.), *Advances in Neural Information Processing Systems*, volume 34, pp. 17480–17492. Curran Associates, Inc., 2021a. URL https://proceedings.neurips.cc/paper_files/paper/2021/file/9219adc5c42107c4911e249155320648-Paper.pdf.

Axel Sauer, Kashyap Chitta, Jens Müller, and Andreas Geiger. Projected gans converge faster, 2021b. URL https://arxiv.org/abs/2111.01007.

Axel Sauer, Katja Schwarz, and Andreas Geiger. Stylegan-xl: Scaling stylegan to large diverse datasets, 2022. URL https://arxiv.org/abs/2202.00273.

Shai Shalev-Shwartz et al. Online learning and online convex optimization. *Foundations and Trends® in Machine Learning*, 4(2):107–194, 2012.

Shashank Singh. Continuum-armed bandits: A function space perspective, 2021. URL https://arxiv.org/abs/2010.08007.

George Stein, Jesse Cresswell, Rasa Hosseinzadeh, Yi Sui, Brendan Ross, Valentin Villecroze, Zhaoyan Liu, Anthony L Caterini, Eric Taylor, and Gabriel Loaiza-Ganem. Exposing flaws of generative model evaluation metrics and their unfair treatment of diffusion models. In *Advances in Neural Information Processing Systems*, volume 36, 2023.

Christian Szegedy, Vincent Vanhoucke, Sergey Ioffe, Jon Shlens, and Zbigniew Wojna. Rethinking the inception architecture for computer vision. In *Proceedings of the IEEE conference on computer vision and pattern recognition*, pp. 2818–2826, 2016.

William R. Thompson. On the likelihood that one unknown probability exceeds another in view of the evidence of two samples. *Biometrika*, 25(3/4):285–294, 1933. ISSN 00063444. URL http://www.jstor.org/stable/2332286.

Hugo Touvron, Thibaut Lavril, Gautier Izacard, Xavier Martinet, Marie-Anne Lachaux, Timothée Lacroix, Baptiste Rozière, Naman Goyal, Eric Hambro, Faisal Azhar, Aurelien Rodriguez, Armand Joulin, Edouard Grave, and Guillaume Lample. Llama: Open and efficient foundation language models, 2023. URL https://arxiv.org/abs/2302.13971.

Steven Walton, Ali Hassani, Xingqian Xu, Zhangyang Wang, and Humphrey Shi. Stylenat: Giving each head a new perspective, 2023. URL https://arxiv.org/abs/2211.05770.

Nir Weinberger and Michal Yemini. Multi-armed bandits with self-information rewards. *IEEE Transactions on Information Theory*, 69(11):7160–7184, 2023. doi: 10.1109/TIT.2023.3299460.

Ceyuan Yang, Yujun Shen, Yinghao Xu, and Bolei Zhou. Data-efficient instance generation from instance discrimination, 2021. URL https://arxiv.org/abs/2106.04566.

Fisher Yu, Ari Seff, Yinda Zhang, Shuran Song, Thomas Funkhouser, and Jianxiong Xiao. Lsun: Construction of a large-scale image dataset using deep learning with humans in the loop, 2016. URL https://arxiv.org/abs/1506.03365.

8 APPENDIX

8.1 PROOF OF THEOREM 1

Consider any $\tilde{x}_{i,a} \in \mathcal{X}$. Let $\tilde{\mathbf{x}}$ be the samples which are identical to $\mathbf{x}$ except that one entry $x_{i,a}$ is changed to $\tilde{x}_{i,a}$. We have

$$\begin{aligned}
&\left|\hat{L}(\boldsymbol{\alpha};\tilde{\mathbf{x}}) - \hat{L}(\boldsymbol{\alpha};\mathbf{x})\right| \\
&= \left| \frac{\alpha_i}{n_i}\left(f(\tilde{x}_{i,a}) - f(x_{i,a})\right) + 2\sum_{(j,b)\neq(i,a)} \frac{\alpha_i\alpha_j}{n_i n_j}\left(\kappa(\tilde{x}_{i,a}, x_{j,b}) - \kappa(x_{i,a}, x_{j,b})\right) \right. \\
&\quad \left. + \frac{\alpha_i^2}{n_i^2}\left(\kappa(\tilde{x}_{i,a}, \tilde{x}_{i,a}) - \kappa(x_{i,a}, x_{i,a})\right) \right| \\
&\leq \frac{\alpha_i}{n_i}\Delta_f + 2\sum_{(j,b)\neq(i,a)} \frac{\alpha_i\alpha_j}{n_i n_j}\Delta_\kappa + \frac{\alpha_i^2}{n_i^2}\Delta_\kappa \\
&\leq \frac{\alpha_i}{n_i}(\Delta_f + 2\Delta_\kappa) \\
&= \frac{\alpha_i}{n_i}\Delta_L.
\end{aligned}$$

By McDiarmid's inequality,

$$\begin{aligned}
\mathbb{P}\left(\hat{L}(\boldsymbol{\alpha};\mathbf{x}) - \mathbb{E}[\hat{L}(\boldsymbol{\alpha};\mathbf{x})] \geq \epsilon\right) &\leq \exp\left(-\frac{2\epsilon^2}{\sum_{i=1}^m \sum_{a=1}^{n_i}(\frac{\alpha_i}{n_i}\Delta_L)^2}\right) \\
&= \exp\left(-\frac{2\epsilon^2}{\Delta_L^2 \sum_{i=1}^m \alpha_i^2/n_i}\right).
\end{aligned}$$

Note that

$$\begin{aligned}
&\left|L(\boldsymbol{\alpha}) - \mathbb{E}[\hat{L}(\boldsymbol{\alpha};\mathbf{x})]\right| \\
&= \left|\mathbb{E}_{X,X'\overset{\text{iid}}{\sim}P}[\kappa(X,X')] - \mathbb{E}\left[\sum_{(i,j)\in[m]^2} \frac{\alpha_i\alpha_j}{n_i n_j}\sum_{a=1}^{n_i}\sum_{b=1}^{n_j}\kappa(x_{i,a}, x_{j,b})\right]\right| \\
&= \left|\sum_{i=1}^m \frac{\alpha_i^2}{n_i^2}\sum_{a=1}^{n_i}\left(\mathbb{E}_{X,X'\overset{\text{iid}}{\sim}P}[\kappa(X,X')] - \mathbb{E}[\kappa(x_{i,a}, x_{i,a})]\right)\right| \\
&\leq \sum_{i=1}^m \frac{\alpha_i^2}{n_i}\Delta_\kappa.
\end{aligned}$$

Hence, for $\delta > 0$,

$$\mathbb{P}\left(\hat{L}(\boldsymbol{\alpha};\mathbf{x}) - L(\boldsymbol{\alpha}) \geq \Delta_L\sqrt{\frac{\log(1/\delta)}{2}\sum_{i=1}^m \frac{\alpha_i^2}{n_i}} + \Delta_\kappa\sum_{i=1}^m \frac{\alpha_i^2}{n_i}\right) \leq \delta.$$

The result follows from

$$\begin{aligned}
&\Delta_L\sqrt{\frac{\log(1/\delta)}{2}\sum_{i=1}^m \frac{\alpha_i^2}{n_i}} + \Delta_\kappa\sum_{i=1}^m \frac{\alpha_i^2}{n_i} \\
&\leq \Delta_L\sum_{i=1}^m \sqrt{\frac{\log(1/\delta)}{2}\frac{\alpha_i^2}{n_i}} + \Delta_\kappa\sum_{i=1}^m \frac{\alpha_i}{n_i} \\
&= \sum_{i=1}^m \left(\Delta_L\sqrt{\frac{\log(1/\delta)}{2n_i}} + \frac{\Delta_\kappa}{n_i}\right)\alpha_i.
\end{aligned}$$

The other direction of the inequality is similar.

8.2 Sparse Mixture Upper Confidence Bound-Continuum-Armed Bandit Algorithm

The optimal mixture may involve a large number of models. It is sometimes of interest to identify a small subset of models that can still give diverse samples. We now consider the scenario where there is a cost associated with each arm. If we have to pay a cost per pull, then this cost can be absorbed into the function f, and the problem reduces to the aforementioned quadratic multi-armed bandit. However, if the cost is a "subscription fee" that we have to pay for each arm at each round, even if we do not pull that arm at that time, until we decide to "unsubscribe" the arm and not pull it anymore, then we have to modify the algorithm to minimize the following average cost

$$L(\hat{P}^{(T)}) + \frac{\lambda}{T}\sum_{i=1}^{m} \max\{t \in [T] : b^{(t)} = i\}, \tag{9}$$

where $\hat{P}^{(T)}$ is the empirical distribution of the first T samples, $b^{(t)}$ is the arm pulled at time t, $\max\{t \in [T] : b^{(t)} = i\}$ is the last time we pull arm i, and λ is the subscription fee per round. Intuitively, we have to subscribe to arm i until the last use time $\max\{t \in [T] : b^{(t)} = i\}$. As $T \to \infty$, we hope that the average cost (9) approaches the optimal cost $\min_{\boldsymbol{\alpha}} (L(\boldsymbol{\alpha}) + \lambda\|\boldsymbol{\alpha}\|_0)$, where $\|\boldsymbol{\alpha}\|_0$ is the number of nonzero entries of $\boldsymbol{\alpha}$. Minimizing (9) allows us to simultaneously select the best subset of arms and the optimal mixture in the long run, akin to variable selection methods in statistical learning.

We now generalize the Mixture-UCB-CAB algorithm to the *sparse mixture upper confidence bound – continuum-armed bandit (Sparse-Mixture-UCB-CAB) algorithm*, which has parameters $\lambda \geq 0$ and $\beta > 1$. This algorithm is inspired by the *backward elimination method* for variable selection (Efroymson, 1960), which starts with all variables and gradually removing variables irrelevant to our prediction. Here, we start with a set of subscribed arms $\mathcal{S}$ that contains all arms $[m]$, and gradually dropping the worst arm i' as long as the upper confidence bound of the optimal cost without arm i' is lower than the lower confidence bound of the optimal cost with arm i', which implies that dropping arm i' will have a high likelihood of reducing the cost. The algorithm is given in Algorithm 3, and the experiments are presented in Appendix 8.3.

Asymptotically, Sparse-Mixture-UCB-CAB attempts to minimize the cost $\min_{\boldsymbol{\alpha}} (L(\boldsymbol{\alpha}) + \lambda\|\boldsymbol{\alpha}\|_0)$. If a fixed sparsity ℓ is desired instead, we can start with $\lambda = 0$, and gradually increase λ at each round until $|\mathcal{S}| = \ell$, and then stop unsubscribing arms.

8.3 Details of the Numerical Experiments

Hyper-parameter Choice. The kernel bandwidths for the RKE and KID metrics were chosen based on the guidelines provided in their respective papers to ensure clear distinction between models. The values for Δ_L and Δ_κ in our online algorithms (7) were set according to the magnitudes of the metrics and their behavior on a validation subset. The number of sampling rounds was adjusted according to the number of arms and metric convergence, both of which depend on the bandwidth. To ensure the statistical significance of results, all experiments were repeated 10 times with different random seeds, and the reported plots represent the average results.

8.3.1 Optimal Mixture for Quality and Diversity via KID

Suppose P is the distribution of generated images of a model, and Q is the target distribution. Recall that for KID (3), we take the quadratic term to be $\kappa(x, x') = k(\psi(x), \psi(x'))$ (with an expectation $\mathbb{E}_{X,X'\sim P}[k(\psi(X), \psi(X'))]$) and the linear term to be $f(x) = -2\mathbb{E}_{Y\sim Q}[k(\psi(x), \psi(Y))]$ (with an expectation $-2\mathbb{E}_{X\sim P, Y\sim Q}[k(\psi(X), \psi(Y))]$). In order to run our online algorithms, we use Δ_L and Δ_κ based on a validation portion to make sure the UCB terms have the right magnitude for forcing exploration.

FFHQ Generated Images. In this experiment, we used images generated by five different models: LDM (Rombach et al., 2022), StyleGAN-XL (Sauer et al., 2022), Efficient-vdVAE (Hazami et al., 2022), Insgen (Yang et al., 2021), and StyleNAT (Walton et al., 2023). We used 10,000 images from each model to determine the optimal mixture, resulting in the weights (0.33, 0.57, 0, 0, 0.10). A

Algorithm 3 Sparse-Mixture-UCB-CAB

Input: m generative arms, number of rounds T
Output: Gathered samples $\mathbf{x}^{(T)}$
Initialize the set of subscribed arms $\mathcal{S} \leftarrow [m]$.
for $t \in \{0, \dots, m-1\}$ **do**
  Pull arm $t+1$ at time $t+1$ to obtain sample $x_{t+1,1} \sim P_{t+1}$. Set $n_{t+1}^{(m)} = 1$.
end for
for $t \in \{m, \dots, T-1\}$ **do**
  repeat
    Compute

$$\boldsymbol{\alpha}^{(t)} \leftarrow \underset{\boldsymbol{\alpha}:\, \mathrm{supp}(\boldsymbol{\alpha}) \subseteq \mathcal{S}}{\mathrm{argmin}} \left(\hat{L}(\boldsymbol{\alpha}; \mathbf{x}^{(t)}) + \lambda |\mathcal{S}| - (\boldsymbol{\epsilon}^{(t)})^\top \boldsymbol{\alpha} \right), \tag{10}$$

    where $\boldsymbol{\epsilon}^{(t)} \in \mathbb{R}^m$ is defined in (7). Let the minimum value above be C.
    Compute the following "worst arm" if $|\mathcal{S}| \geq 2$:

$$i' \leftarrow \underset{i \in \mathcal{S}}{\mathrm{argmin}} \min_{\boldsymbol{\alpha}:\, \mathrm{supp}(\boldsymbol{\alpha}) \subseteq \mathcal{S} \setminus \{i\}} \left(\hat{L}(\boldsymbol{\alpha}; \mathbf{x}^{(t)}) + \lambda(|\mathcal{S}| - 1) + (\boldsymbol{\epsilon}^{(t)})^\top \boldsymbol{\alpha} \right).$$

    Let the minimum value above be C'.
    if $C' \leq C$ **then**
      Unsubscribe arm i' (i.e., $\mathcal{S} \leftarrow \mathcal{S} \setminus \{i'\}$)
    end if
  until no more arms are unsubscribed
  Generate the arm index $b^{(t+1)} \in [m]$ at random with $\mathbb{P}(b^{(t+1)} = i) = \alpha_i^{(t)}$.
  Pull arm $b = b^{(t+1)}$ at time $t+1$ to obtain a new sample $x_{b, n_b^{(t)}+1} \sim P_b$. Set $n_b^{(t+1)} = n_b^{(t)} + 1$ and $n_j^{(t+1)} = n_j^{(t)}$ for $j \neq b$.
end for
return samples $\mathbf{x}^{(T)}$

kernel bandwidth of 40 was used for calculating the RKE, and the online algorithms were run for 8,000 sampling rounds. The quality and diversity scores for each model, including the results for the optimal mixture based on KID, are presented in Table 1.

In Tables 1 and 2, we observe that the Precision of the optimal mixture is similar to that of the maximum Precision score among individual models. On the other hand, the Recall-based diversity improved in the mixture case. However, the quality-measuring Density score slightly decreased for the selected mixture model, as Density is a linear score for quality that could be optimized by an individual model. On the other hand, the Coverage score of the mixture model was higher than each individual model.

Note that Precision and Density are scores on the average quality of samples. Intuitively, the quality score of a mixture of models is the average of the quality score of the individual models, and hence the quality score of a mixture cannot be better than the best individual model. On the other hand, Recall and Coverage measure the diversity of the samples, which can increase by considering a mixture of the models. To evaluate the net diversity-quality effect, we measured the FID score of the selected mixture and the best individual model, and the selected mixture model had a better FID score compared to the individual model with the best FID.

LSUN-Bedroom We used images generated by four different models: StyleGAN (Karras et al., 2019a), Projected GAN (Sauer et al., 2021a), iDDPM (Nichol & Dhariwal, 2021), and Unleashing Transformers (Bond-Taylor et al., 2021). We utilized 10,000 images from each model to compute the optimal mixture, resulting in weights of (0.51, 0, 0.49, 0). A kernel bandwidth of 40 was applied, and the algorithm was run for 8,000 sampling steps. The quality and diversity scores for each model, including the results for the optimal mixture based on KID, are presented in Table 2.

Model	Precision ↑	Recall ↑	Density ↑	Coverage ↑	FID ↓
LDM	0.856 ± 0.008	0.482 ± 0.008	0.959 ± 0.027	0.776 ± 0.006	189.876 ± 1.976
StyleGAN-XL	0.798 ± 0.007	0.515 ± 0.007	0.726 ± 0.018	0.691 ± 0.009	186.163 ± 2.752
Efficient-vdVAE	0.854 ± 0.011	0.143 ± 0.007	0.952 ± 0.033	0.545 ± 0.008	490.385 ± 4.377
Insgen	0.76 ± 0.006	0.281 ± 0.007	0.716 ± 0.016	0.692 ± 0.005	278.235 ± 1.617
StyleNAT	0.834 ± 0.008	0.478 ± 0.007	0.867 ± 0.023	0.775 ± 0.007	185.067 ± 2.123
Optimal Mixture (KID)	0.818 ± 0.007	0.57 ± 0.008	0.816 ± 0.025	0.765 ± 0.007	168.127 ± 1.596

Table 1: Quality and diversity scores for the FFHQ experiment, including precision, recall, density, coverage, and FID metrics (± standard deviation).

Model	Precision ↑	Recall ↑	Density ↑	Coverage ↑	FID ↓
StyleGAN	0.838 ± 0.008	0.446 ± 0.007	0.941 ± 0.019	0.821 ± 0.004	175.575 ± 2.055
Projected GAN	0.749 ± 0.015	0.329 ± 0.008	0.592 ± 0.027	0.517 ± 0.008	324.066 ± 3.753
iDDPM	0.838 ± 0.006	0.641 ± 0.006	0.660 ± 0.018	0.825 ± 0.006	154.680 ± 3.036
Unleashing Transformers	0.786 ± 0.008	0.449 ± 0.006	0.649 ± 0.013	0.581 ± 0.013	339.982 ± 6.118
Optimal Mixture (KID)	0.838 ± 0.006	0.589 ± 0.005	0.900 ± 0.016	0.833 ± 0.004	149.779 ± 2.238

Table 2: Quality and diversity scores for the LSUN-Bedroom experiment, including precision, recall, density, coverage, and FID metrics (± standard deviation).

Truncated FFHQ. We used StyleGAN2-ADA (Karras et al., 2020) trained on FFHQ dataset to generate images. We randomly chose 8 initial points and used the Truncation Method (Marchesi, 2017; Karras et al., 2019b) to generate images with limited diversity around each of the chosen points. We used truncation value of 0.3 and generated 5000 images from each model to find the optimal mixture. The weights for the mixture was (0.07, 0.28, 0.10, 0.04, 0.21, 0.11, 0.12, 0.07). A kernel bandwidth of 40 was used, and 4,000 sampling steps were conducted.

8.3.2 Optimal Mixture for Diversity via RKE

Truncated FFHQ. We employed StyleGAN2-ADA (Karras et al., 2020), trained on the FFHQ dataset, to generate images. Eight initial points were randomly selected, and the Truncation Method (Marchesi, 2017; Karras et al., 2019b) was applied with a truncation value of 0.3 to generate images with limited diversity around these points. For the quadratic optimization, 5,000 images were generated from each model, using a kernel bandwidth of 40 to identify the optimal mixture. In the online experiment, a new set of generated images was used, and sampling was conducted over 2,000 steps.

Truncated AFHQ Cat. Similar to the previous experiment, we used StyleGAN2-ADA to generate AFHQ Cat images. Four initial points were selected, and a truncation value of 0.6 was applied to simulate diversity-controlled models. For the quadratic optimization, 5,000 images were generated from each model, with sampling conducted over 1,200 steps to determine the optimal mixture.

Style-Specific Generators. We used Stable Diffusion XL to generate images of cars in distinct styles: realistic, surreal, and cartoon. For this experiment, we utilized 2,000 images from each model to determine the optimal mixture, which yielded weights of (0.67, 0.27, 0.06). This mixture increased the RKE value from 7.8 (the optimal value of the realistic images) to 9.2. We set the kernel bandwidth to 30 and executed the online algorithms over 1,000 sampling steps.

Sofa Images. We generated images of the object "Sofa" using prompts with environmental descriptions across the models FLUX.1-Schnell (Lab, 2024), Kandinsky 3.0 (Arkhipkin et al., 2023), PixArt-α (Chen et al., 2023a), and Stable Diffusion XL (Podell et al., 2023). Solving the RKE optimization with 1,000 images revealed that sampling 38% from FLUX and 62% from Kandinsky improved the RKE score from the one-arm optimum of 7.21 to 7.57. We set the kernel bandwidth to 30 and conducted the online experiment over 700 steps. We observed that Mixture-UCB-OGD achieved noticeably faster convergence to the optimal mixture RKE in this scenario.

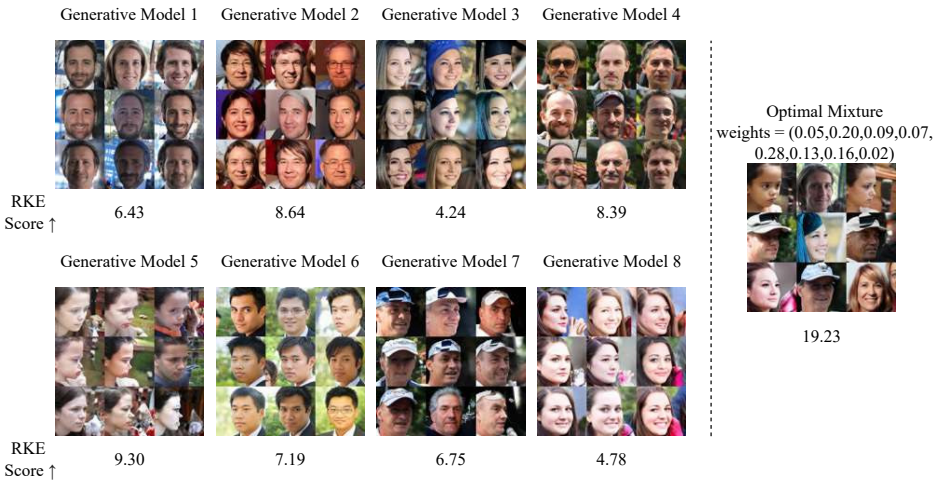

Figure 7: Visual demonstration of the increase in diversity when mixing arms compared to individual arms for truncated FFHQ generative models. The RKE values for each model and the mixture serve as indicators of diversity.

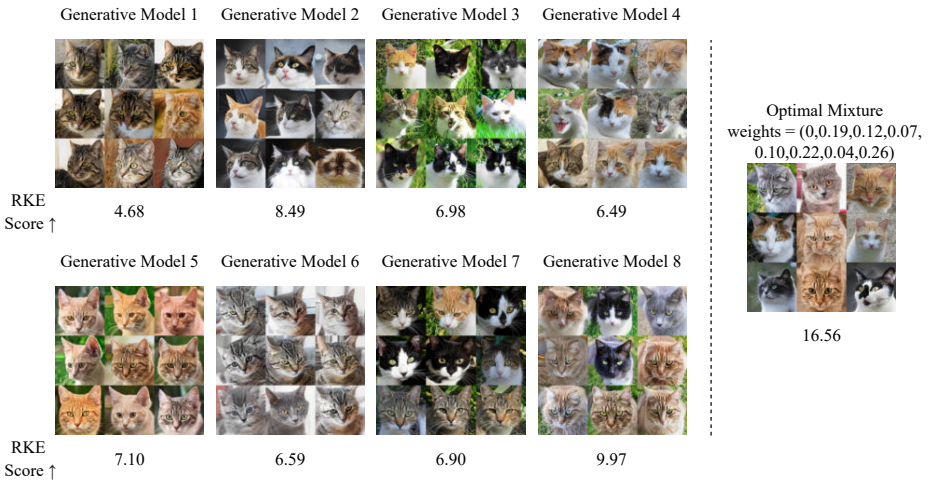

Figure 8: Visual demonstration of the increase in diversity when mixing arms compared to individual arms for truncated AFHQ Cat generative models. The RKE values for each model and the mixture represent the diversity.

The prompts followed the structure: "A *adjective* sofa is *verb* in a *location*," with the terms for Adjective, Action, and Location generated by GPT-4o (OpenAI, 2024), specifically for the object "Sofa."

Dog Breeds Images. Stable Diffusion XL was used to generate images of three dog breeds: Poodle, Bulldog, and German Shepherd. As shown in Figure 4, using a mixture of models resulted in an increase in mode count from 1.5 to 3, supporting our claim of enhanced diversity. We set the kernel bandwidth to 50 and generated 1,000 images for each breed to determine the optimal mixture, which was (0.33, 0.31, 0.36). Additionally, the online algorithms were executed for 500 sampling steps.

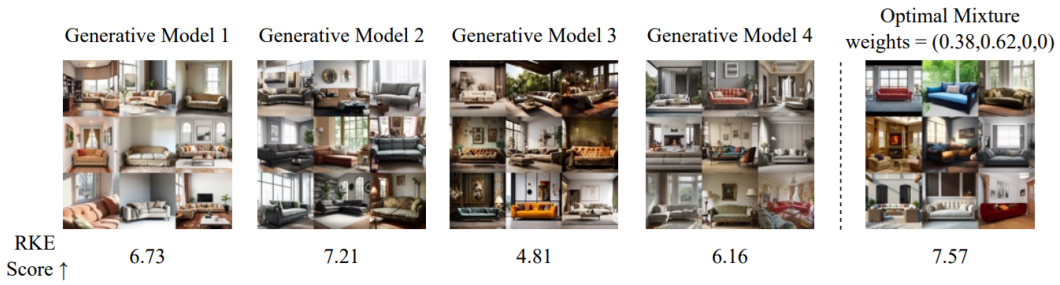

Figure 9: Visual comparison of diversity of each arm and the mixture for sofa image generators

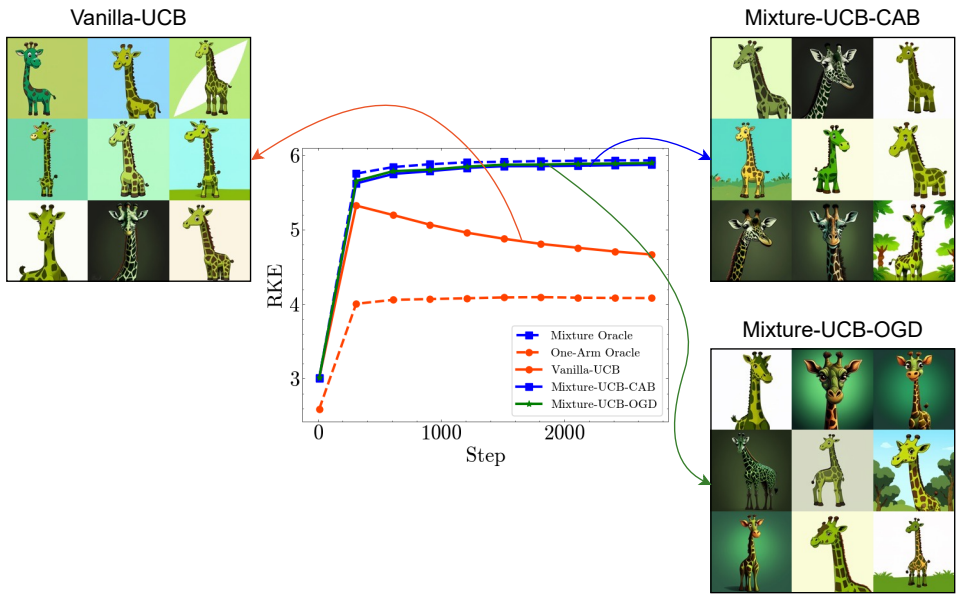

Figure 10: Comparison of samples generated using our proposed algorithms Mixture-UCB-CAB and Mixture-UCB-OGD with the baseline one-arm online algorithm

Giraffe Images. We used three models—Stable Diffusion 3-medium (Esser et al., 2024), Kandinsky 3 (Arkhipkin et al., 2024), and PixArt-α (Chen et al., 2023a)—to generate 5000 images each using the prompt: "Dark green giraffe, detailed, cartoon style." In Fig. 1, we observe that while each model adheres to the prompt, they fail to generate a diverse set of images. In contrast, the mixture demonstrates noticeably greater diversity, as evident both visually and quantitatively from the RKE (Jalali et al., 2023) and Vendi (Friedman & Dieng, 2023) scores. Furthermore, in Fig. 10, we observe that the last nine samples generated by our online algorithm at step 1500 are significantly more diverse compared to those generated by the Vanilla-UCB algorithm.

Text Generative Models We utilized the OpenLLMText dataset (Chen et al., 2023b), which consists of 60,000 human texts rephrased paragraph by paragraph using the models GPT2-XL (Radford et al., 2019), LLaMA-7B (Touvron et al., 2023), and PaLM (Chowdhery et al., 2022). To extract features from each text, we employed the RoBERTa text encoder (Liu et al., 2019). By solving the optimization problem on 10,000 texts from each model, we found that mixing the models with probabilities (0.02, 0.34, 0.64, 0) achieved the optimal mixture, improving the RKE from an optimal single model score of 69.3 to 75.2. A bandwidth of 0.6 was used for the kernel, and we ran the online algorithms for 7,000 steps to demonstrate their performance.

Sparse Mixture Four different initial points and StyleGAN2-ADA were used to generate images with a truncation of 0.6 around the points, simulating diversity-controlled arms. A value of $\lambda = 0.06$ and a bandwidth of 30 were selected based on the magnitudes of RKEs from the validation dataset to

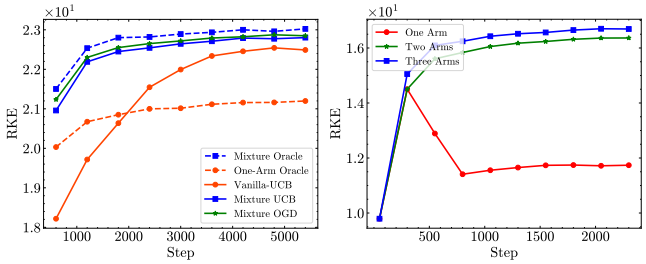

(a) Text generators (b) Sparse mixture

Figure 11: Comparison of online algorithms for the RKE metric on text generative models and the Sparse Mixture algorithm for FFHQ truncated generators

determine when to "unsubscribe" arms in the Sparse-Mixure-UCB-CAB algorithm. We conducted three scenarios, gradually reducing the number of arms to between one and three, and presented a comparison of the resulting plots and their convergence values in Figure 11b.

8.3.3 Optimal Mixture for Diversity and Quality via RKE and Precision/Density

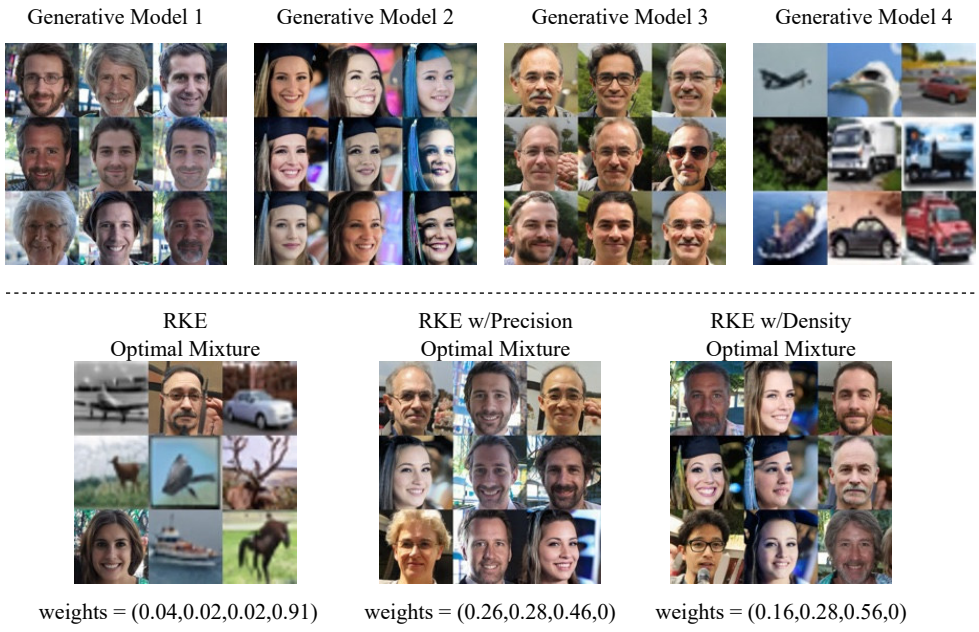

Figure 12: Visual demonstration of the effect of combining Precision/Density with RKE. The CIFAR10 generator is excluded when these quality metrics are applied.

In this experiment, we utilized four arms: three of them are StyleGAN2-ADA models trained on FFHQ, each using a truncation value of 0.3 around a randomly selected point. The fourth arm is StyleGAN2-ADA trained on CIFAR-10. We generated 5,000 images and used a kernel bandwidth of 30 to calculate the optimal mixture. When optimizing purely for diversity using the RKE metric, the high diversity of the fourth arm leads to a probability of 0.91 being assigned to it, as shown in Figure 12. However, despite the increased diversity, the quality of the generated images, based on the reference distribution, is unsatisfactory.

To address this, we incorporate a quality metric, specifically Precision/Density, into the optimization. We subtract the weighted Precision/Density from the RKE value, ensuring a balance between quality and diversity. The weight for the quality metric ($\lambda = 0.2$) was selected based on validation data to ensure comparable scaling between the two metrics. As a result, Figure 12 shows that the fourth arm, which had low-quality outputs, is assigned a weight of zero.

We use the RKE score as $\mathbf{K}$ and the weighted Precision/Density as $\mathbf{f}$ according to equation 5. The online algorithms were run for 4,000 steps, with the results depicted in Figure 6.

8.4 Proof of Theorem 2

Before we prove Theorem 2, we first prove a worst case concentration bound.

Lemma 1 *Let $T \geq 2$, and $x_{i,1}, x_{i,2}, \ldots \overset{\text{iid}}{\sim} P_i$ for $i \in [m]$. Let $\Delta_L := 2\Delta_\kappa + \Delta_f$. For $n_1, \ldots, n_m \in [T]$, let $\mathbf{x}^{(n_i)_i} := (x_{i,a})_{i\in[m],\, a\in[n_i]}$. Fix any $\delta > 0$. With probability at least $1-\delta$, we have*

$$L(\boldsymbol{\alpha}) - \hat{L}(\boldsymbol{\alpha}; \mathbf{x}^{(n_i)_i}) \leq \sum_{i=1}^{m} \left(\Delta_L \sqrt{\frac{1}{2n_i} \log \frac{m^2 T^2}{2\delta}} + \frac{\Delta_\kappa}{n_i} \right) \alpha_i.$$

for every $n_1, \ldots, n_m \in [T]$ and probability vector $\boldsymbol{\alpha}$. The same holds for $\hat{L}(\boldsymbol{\alpha}; \mathbf{x}^{(n_i)_i}) - L(\boldsymbol{\alpha})$ instead of $L(\boldsymbol{\alpha}) - \hat{L}(\boldsymbol{\alpha}; \mathbf{x}^{(n_i)_i})$.

Proof: Fix any $n_1, \ldots, n_m \in [T]$, and write $\mathbf{x} = \mathbf{x}^{(n_i)_i}$. We have

$$L(\boldsymbol{\alpha}) - \hat{L}(\boldsymbol{\alpha}; \mathbf{x}) = \sum_{i,j} \alpha_i \alpha_j \left(\frac{\mathbf{f}_i + \mathbf{f}_j}{2} + \mathbf{K}_{i,j} - \frac{\hat{\mathbf{f}}_i(\mathbf{x}) + \hat{\mathbf{f}}_j(\mathbf{x})}{2} - \hat{\mathbf{K}}_{i,j}(\mathbf{x}) \right).$$

For $i = j$, applying Theorem 1 on $\boldsymbol{\alpha}$ being the i-th basis vector,

$$\mathbb{P}\left(\mathbf{f}_i + \mathbf{K}_{i,i} - \hat{\mathbf{f}}_i(\mathbf{x}) - \hat{\mathbf{K}}_{i,i}(\mathbf{x}) \geq \Delta_L \sqrt{\frac{\log(1/\delta)}{2n_i}} + \frac{\Delta_\kappa}{n_i} \right) \leq \delta. \tag{11}$$

For $i \neq j$, we will use similar arguments as Theorem 1. Let $\tilde{\mathbf{x}}$ be the samples which are identical to $\mathbf{x}$ except that one entry $x_{i,a}$ of the i-th arm is changed to $\tilde{x}_{i,a}$. We have

$$\begin{aligned}
&\left| \frac{\hat{\mathbf{f}}_i(\tilde{\mathbf{x}}) + \hat{\mathbf{f}}_j(\tilde{\mathbf{x}})}{2} + \hat{\mathbf{K}}_{i,j}(\tilde{\mathbf{x}}) - \frac{\hat{\mathbf{f}}_i(\mathbf{x}) + \hat{\mathbf{f}}_j(\mathbf{x})}{2} - \hat{\mathbf{K}}_{i,j}(\mathbf{x}) \right| \\
&= \left| \frac{1}{2n_i} \left(f(\tilde{x}_{i,a}) - f(x_{i,a}) \right) + \frac{1}{n_i n_j} \sum_{b=1}^{n_j} \left(\kappa(\tilde{x}_{i,a}, x_{j,b}) - \kappa(x_{i,a}, x_{j,b}) \right) \right| \\
&\leq \frac{\Delta_f}{2n_i} + \frac{\Delta_\kappa}{n_i} \\
&= \frac{\Delta_L}{2n_i}.
\end{aligned}$$

Note that $\mathbb{E}[\frac{\hat{\mathbf{f}}_i(\mathbf{x}) + \hat{\mathbf{f}}_j(\mathbf{x})}{2} + \hat{\mathbf{K}}_{i,j}(\mathbf{x})] = \frac{\mathbf{f}_i + \mathbf{f}_j}{2} - \mathbf{K}_{i,j}$. By McDiarmid's inequality,

$$\begin{aligned}
&\mathbb{P}\left(\frac{\mathbf{f}_i + \mathbf{f}_j}{2} + \mathbf{K}_{i,j} - \frac{\hat{\mathbf{f}}_i(\mathbf{x}) + \hat{\mathbf{f}}_j(\mathbf{x})}{2} - \hat{\mathbf{K}}_{i,j}(\mathbf{x}) \geq \epsilon \right) \\
&\leq \exp\left(- \frac{2\epsilon^2}{n_i \left(\frac{\Delta_L}{2n_i} \right)^2 + n_j \left(\frac{\Delta_L}{2n_j} \right)^2} \right) \\
&= \exp\left(- \frac{8\epsilon^2}{\Delta_L^2 \left(n_i^{-1} + n_j^{-1} \right)} \right).
\end{aligned}$$

Hence,

$$\mathbb{P}\left(\frac{\mathbf{f}_i+\mathbf{f}_j}{2}+\mathbf{K}_{i,j}-\frac{\hat{\mathbf{f}}_i(\mathbf{x})+\hat{\mathbf{f}}_j(\mathbf{x})}{2}-\hat{\mathbf{K}}_{i,j}(\mathbf{x})\geq\Delta_L\sqrt{\frac{\log(1/\delta)}{8}\left(n_i^{-1}+n_j^{-1}\right)}\right)\leq\delta. \tag{12}$$

Note that the event in (11) does not depend on $n_{i'}$ for $i'\neq i$, and the event in (12) does not depend on $n_{i'}$ for $i'\notin\{i,j\}$. By union bound, all the events in (11) and (12) do not hold for all $i\leq j$ and $n_1,\ldots,n_m\in[T]$ with probability at least

$$1-mT\delta-\frac{m(m-1)}{2}T^2\delta\geq 1-\frac{m^2}{2}T^2\delta.$$

If these events do not hold, then

$$\begin{aligned}
&L(\boldsymbol{\alpha})-\hat{L}(\boldsymbol{\alpha};\mathbf{x})\\
&=\sum_{i,j}\alpha_i\alpha_j\left(\frac{\mathbf{f}_i+\mathbf{f}_j}{2}+\mathbf{K}_{i,j}-\frac{\hat{\mathbf{f}}_i(\mathbf{x})+\hat{\mathbf{f}}_j(\mathbf{x})}{2}-\hat{\mathbf{K}}_{i,j}(\mathbf{x})\right)\\
&\leq\sum_i\alpha_i^2\left(\Delta_L\sqrt{\frac{\log(1/\delta)}{2n_i}}+\frac{\Delta_\kappa}{n_i}\right)+\sum_{(i,j)\in[m]^2,i\neq j}\alpha_i\alpha_j\Delta_L\sqrt{\frac{\log(1/\delta)}{8}\left(n_i^{-1}+n_j^{-1}\right)}\\
&\leq\sum_i\alpha_i^2\left(\Delta_L\sqrt{\frac{\log(1/\delta)}{2n_i}}+\frac{\Delta_\kappa}{n_i}\right)+\Delta_L\sqrt{\frac{\log(1/\delta)}{8}}\sum_{(i,j)\in[m]^2,i\neq j}\alpha_i\alpha_j\left(n_i^{-1/2}+n_j^{-1/2}\right)\\
&=\sum_i\alpha_i^2\frac{\Delta_\kappa}{n_i}+\Delta_L\sqrt{\frac{\log(1/\delta)}{8}}\sum_{(i,j)\in[m]^2}\alpha_i\alpha_j\left(n_i^{-1/2}+n_j^{-1/2}\right)\\
&=\sum_i\alpha_i^2\frac{\Delta_\kappa}{n_i}+\Delta_L\sqrt{\frac{\log(1/\delta)}{2}}\sum_i\alpha_i n_i^{-1/2}\\
&\leq\sum_i\left(\Delta_L\sqrt{\frac{\log(1/\delta)}{2n_i}}+\frac{\Delta_\kappa}{n_i}\right)\alpha_i.
\end{aligned}$$

The other direction of the inequality is similar.

We finally prove Theorem 2.

Proof: Assume $m\geq 2$, $\beta\geq 4$ and $T\geq 2$. If $T\leq 40m$, then since $T^{-1}\log T$ is decreasing for $T\geq 3$ (the following inequalities are obviously true for $T=2$),

$$\sqrt{\frac{\beta m\log T}{T}}\geq\sqrt{\frac{4m\log(40m)}{40m}}\geq\sqrt{\frac{\log 80}{10}}\geq 0.66,$$

and Theorem 2 is trivially true since $\mathbb{E}\big[L(\hat{P}^{(T)})\big]-\min_{\boldsymbol{\alpha}}L(\boldsymbol{\alpha})\leq\Delta_L$. Hence we can assume $T\geq 40m+1$.

Let $\boldsymbol{\alpha}^*$ be the minimizer of $L(\boldsymbol{\alpha})$. Let $\bar{x}^{(t)}$ be the sample obtained at the t-th pull. Let $\alpha_i^{(t-1)}=\mathbf{1}\{t=i\}$ for $t\in[m]$, so "$\bar{x}^{(t)}$ is generated from the distribution P_i with probability $\alpha_i^{(t-1)}$" holds for every $t\geq 1$. Write $\bar{x}^{([s])}:=(\bar{x}^{(t)})_{t\in[s]}$. For $s<t$, let $\hat{x}^{(s)}$ be a random variable with the same conditional distribution given $\bar{x}^{([s-1])}$ as $\bar{x}^{(s)}$, but is conditionally independent of all other random variables given $\bar{x}^{([s-1])}$. The joint distribution of $\bar{x}^{([t-1])},\bar{x}^{(t)},\hat{x}^{(s)}$ is

$$P_{\bar{x}^{([t-1])},\bar{x}^{(t)},\hat{x}^{(s)}}=P_{\bar{x}^{([t-1])},\bar{x}^{(t)}}P_{\bar{x}^{(s)}|\bar{x}^{([s-1])}}.$$

Recall that $\bar{x}^{(s)}$ is generated from the distribution P_i with probability $\alpha_i^{(s-1)}$ for $i \in [m]$, where $\boldsymbol{\alpha}^{(s-1)} = (\alpha_i^{(s-1)})_{i\in[m]}$ is computed using $\bar{x}^{([s-1])}$. We have

$$\begin{aligned}
&\mathbb{E}[\kappa(\hat{x}^{(s)}, \bar{x}^{(t)})] \\
&= \mathbb{E}\left[\mathbb{E}\left[\kappa(\hat{x}^{(s)}, \bar{x}^{(t)}) \,\middle|\, \bar{x}^{([t-1])}\right]\right] \\
&\overset{(a)}{=} \mathbb{E}\left[\sum_{i=1}^{m}\sum_{j=1}^{m} \alpha_i^{(s-1)}\alpha_i^{(t-1)} \mathbb{E}_{X\sim P_i, X'\sim P_j}\left[\kappa(X, X')\right]\right] \\
&= \mathbb{E}\left[(\boldsymbol{\alpha}^{(s-1)})^\top \mathbf{K} \boldsymbol{\alpha}^{(t-1)}\right],
\end{aligned}$$

where (a) is because $\hat{x}^{(s)}$ only depends on $\bar{x}^{([s-1])}$ (i.e., is conditionally independent of all other random variables in the expression given $\bar{x}^{([s-1])}$), and $\bar{x}^{(t)}$ only depends on $\bar{x}^{([t-1])}$. Write $\delta_{\mathrm{TV}}(A\|B)$ for the total variation distance between the distributions of the random variables A and B. Write $I(A; B|C)$ for the conditional mutual information between A and B given C in nats. We have

$$\begin{aligned}
&\mathbb{E}[\kappa(\bar{x}^{(s)}, \bar{x}^{(t)})] \\
&\overset{(b)}{\le} \mathbb{E}[\kappa(\hat{x}^{(s)}, \bar{x}^{(t)})] + \Delta_\kappa \delta_{\mathrm{TV}}(\bar{x}^{(s)}, \bar{x}^{(t)} \,\|\, \hat{x}^{(s)}, \bar{x}^{(t)}) \\
&\le \mathbb{E}\left[(\boldsymbol{\alpha}^{(s-1)})^\top \mathbf{K} \boldsymbol{\alpha}^{(t-1)}\right] + \Delta_\kappa \delta_{\mathrm{TV}}(\bar{x}^{([s-1])}, \bar{x}^{(s)}, \bar{x}^{(t)} \,\|\, \bar{x}^{([s-1])}, \hat{x}^{(s)}, \bar{x}^{(t)}) \\
&\overset{(c)}{\le} \mathbb{E}\left[(\boldsymbol{\alpha}^{(s-1)})^\top \mathbf{K} \boldsymbol{\alpha}^{(t-1)}\right] + \Delta_\kappa \sqrt{\frac{1}{2} I(\bar{x}^{(s)}; \bar{x}^{(t)} | \bar{x}^{([s-1])})},
\end{aligned}$$

where (b) is because κ takes values over $[\kappa_0, \kappa_1]$ with $\Delta_\kappa = \kappa_1 - \kappa_0$, and (c) is by Pinsker's inequality. We also have, for every t,

$$\mathbb{E}[\kappa(\bar{x}^{(t)}, \bar{x}^{(t)})] \le \mathbb{E}\left[(\boldsymbol{\alpha}^{(t-1)})^\top \mathbf{K} \boldsymbol{\alpha}^{(t-1)}\right] + \Delta_\kappa.$$

Hence,

$$\begin{aligned}
&\mathbb{E}\left[\frac{1}{T^2}\sum_{s=1}^{T}\sum_{t=1}^{T} \kappa(\bar{x}^{(s)}, \bar{x}^{(t)})\right] - \mathbb{E}\left[\frac{1}{T^2}\sum_{s=1}^{T}\sum_{t=1}^{T} (\boldsymbol{\alpha}^{(s-1)})^\top \mathbf{K} \boldsymbol{\alpha}^{(t-1)}\right] \\
&\le \frac{2\Delta_\kappa}{T^2}\sum_{s=1}^{T}\sum_{t=s+1}^{T} \sqrt{\frac{1}{2} I(\bar{x}^{(s)}; \bar{x}^{(t)} | \bar{x}^{([s-1])})} + \frac{\Delta_\kappa}{T} \\
&= \frac{2\Delta_\kappa}{T^2}\sum_{t=1}^{T}\sum_{s=1}^{t-1} \sqrt{\frac{1}{2} I(\bar{x}^{(s)}; \bar{x}^{(t)} | \bar{x}^{([s-1])})} + \frac{\Delta_\kappa}{T} \\
&\le \frac{2\Delta_\kappa}{T^2}\sum_{t=1}^{T} \sqrt{\frac{t-1}{2}\sum_{s=1}^{t-1} I(\bar{x}^{(s)}; \bar{x}^{(t)} | \bar{x}^{([s-1])})} + \frac{\Delta_\kappa}{T} \\
&\overset{(d)}{=} \frac{2\Delta_\kappa}{T^2}\sum_{t=1}^{T} \sqrt{\frac{t-1}{2} I(\bar{x}^{([t-1])}; \bar{x}^{(t)})} + \frac{\Delta_\kappa}{T} \\
&\overset{(e)}{\le} \frac{2\Delta_\kappa}{T^2}\sum_{t=1}^{T} \sqrt{\frac{t-1}{2}\log m} + \frac{\Delta_\kappa}{T} \\
&\le \frac{2\Delta_\kappa}{T^2}\sqrt{\frac{\log m}{2}} \int_0^T \sqrt{\tau}\mathrm{d}\tau + \frac{\Delta_\kappa}{T} \\
&= \frac{4\Delta_\kappa}{3}\sqrt{\frac{\log m}{2T}} + \frac{\Delta_\kappa}{T},
\end{aligned}$$

where (d) is by the chain rule of mutual information, and (e) is because $\bar{x}^{(t)}$ only depends on $\bar{x}^{([t-1])}$ through the choice of arm $b^{(t)} \in [m]$, and hence $I(\bar{x}^{([t-1])}; \bar{x}^{(t)})$ is upper bounded by the entropy of

$b^{(t)}$, which is at most $\log m$. Also note that $\mathbb{E}[f(\bar{x}^{(t)})] = \mathbf{f}^\top \mathbb{E}[\boldsymbol{\alpha}^{(t-1)}]$. Hence,

$$\begin{aligned}
&\mathbb{E}[L(\hat{P}^{(T)})] \\
&= \mathbb{E}\left[\frac{1}{T}\sum_{t=1}^{T} f(\bar{x}^{(t)}) + \frac{1}{T^2}\sum_{s=1}^{T}\sum_{t=1}^{T}\kappa(\bar{x}^{(s)}, \bar{x}^{(t)})\right] \\
&\leq \mathbb{E}\left[\frac{1}{T}\sum_{t=1}^{T}\mathbf{f}^\top\boldsymbol{\alpha}^{(t-1)} + \frac{1}{T^2}\sum_{s=1}^{T}\sum_{t=1}^{T}(\boldsymbol{\alpha}^{(s-1)})^\top\mathbf{K}\boldsymbol{\alpha}^{(t-1)}\right] + \frac{4\Delta_\kappa}{3}\sqrt{\frac{\log m}{2T}} + \frac{\Delta_\kappa}{T} \\
&= \mathbb{E}\left[\mathbf{f}^\top\frac{1}{T}\sum_{t=1}^{T}\boldsymbol{\alpha}^{(t-1)} + \left(\frac{1}{T}\sum_{t=1}^{T}\boldsymbol{\alpha}^{(t-1)}\right)^\top\mathbf{K}\left(\frac{1}{T}\sum_{t=1}^{T}\boldsymbol{\alpha}^{(t-1)}\right)\right] + \frac{4\Delta_\kappa}{3}\sqrt{\frac{\log m}{2T}} + \frac{\Delta_\kappa}{T} \\
&= \mathbb{E}\left[L\left(\frac{1}{T}\sum_{t=1}^{T}\boldsymbol{\alpha}^{(t-1)}\right)\right] + \frac{4\Delta_\kappa}{3}\sqrt{\frac{\log m}{2T}} + \frac{\Delta_\kappa}{T} \\
&\overset{(f)}{\leq} \frac{1}{T}\sum_{t=1}^{T}\mathbb{E}\left[L(\boldsymbol{\alpha}^{(t-1)})\right] + \frac{4\Delta_\kappa}{3}\sqrt{\frac{\log m}{2T}} + \frac{\Delta_\kappa}{T},
\end{aligned} \tag{13}$$

where (f) is because $\mathbf{K}$ is positive semidefinite, and hence L is convex. Therefore, to bound the optimality gap, we study the expected loss $\mathbb{E}\left[L(\boldsymbol{\alpha}^{(t)})\right]$ of the estimate of the optimal mixture distribution $\boldsymbol{\alpha}^{(t)}$.

Let $\tilde{\delta} > 0$. Let $\tilde{E}$ be the event

$$L(\boldsymbol{\alpha}) - \hat{L}(\boldsymbol{\alpha}; \mathbf{x}^{(n_i)_i}) \leq \sum_{i=1}^{m}\left(\Delta_L\sqrt{\frac{1}{2n_i}\log\frac{m^2T^2}{2\tilde{\delta}}} + \frac{\Delta_\kappa}{n_i}\right)\alpha_i$$

for every $n_1, \ldots, n_m \in [T]$ and probability vector $\boldsymbol{\alpha}$, as in Lemma 1. By Lemma 1, $\mathbb{P}(\tilde{E}) \geq 1 - \tilde{\delta}$.

Fix a time $t \in \{m, \ldots, T\}$. Let E_t be the event

$$\hat{L}(\boldsymbol{\alpha}^*; \mathbf{x}^{(n_i)_i}) - L(\boldsymbol{\alpha}^*) \leq \sum_{i=1}^{m}\left(\Delta_L\sqrt{\frac{\beta\log t}{2n_i}} + \frac{\Delta_\kappa}{n_i}\right)\alpha_i^*$$

for every $n_1, \ldots, n_m \geq 1$ such that $\sum_i n_i = t$. Since

$$\begin{aligned}
&\sum_{i=1}^{m}\left(\Delta_L\sqrt{\frac{1}{2n_i}\log\frac{m^2t^2}{2m^2t^{-2}/2}} + \frac{\Delta_\kappa}{n_i}\right)\alpha_i^* \\
&= \sum_{i=1}^{m}\left(\Delta_L\sqrt{\frac{1}{2n_i}\log t^4} + \frac{\Delta_\kappa}{n_i}\right)\alpha_i^* \\
&\leq \sum_{i=1}^{m}\left(\Delta_L\sqrt{\frac{\beta\log t}{2n_i}} + \frac{\Delta_\kappa}{n_i}\right)\alpha_i^*
\end{aligned}$$

by $\beta \geq 4$, applying Lemma 1,

$$\mathbb{P}(E_t) \geq 1 - m^2t^{-2}/2. \tag{14}$$

If the event E_t holds, by taking $n_i = n_i^{(t)}$,

$$\hat{L}(\boldsymbol{\alpha}^*; \mathbf{x}^{(t)}) - L(\boldsymbol{\alpha}^*) \leq (\boldsymbol{\epsilon}^{(t)})^\top\boldsymbol{\alpha}^*. \tag{15}$$

If the event $\tilde{E}$ holds,

$$\begin{aligned}
&L(\boldsymbol{\alpha}) - \hat{L}(\boldsymbol{\alpha}; \mathbf{x}^{(t)}) \\
&\leq \sum_{i=1}^{m}\left(\Delta_L\sqrt{\frac{1}{2n_i^{(t)}}\log\frac{m^2T^2}{2\tilde{\delta}}} + \frac{\Delta_\kappa}{n_i^{(t)}}\right)\alpha_i
\end{aligned} \tag{16}$$

for every $\boldsymbol{\alpha}$. Combining (15) and (16) (with $\boldsymbol{\alpha} = \boldsymbol{\alpha}^{(t)}$),

$$\begin{aligned}
&\hat{L}(\boldsymbol{\alpha}^{(t)}; \mathbf{x}^{(t)}) - \hat{L}(\boldsymbol{\alpha}^*; \mathbf{x}^{(t)}) + (\boldsymbol{\epsilon}^{(t)})^\top \boldsymbol{\alpha}^* \\
&+ \sum_{i=1}^{m} \left(\Delta_L \sqrt{\frac{1}{2n_i^{(t)}} \log \frac{m^2 T^2}{2\tilde{\delta}}} + \frac{\Delta_\kappa}{n_i^{(t)}} \right) \alpha_i^{(t)} \\
&\geq L(\boldsymbol{\alpha}^{(t)}) - L(\boldsymbol{\alpha}^*).
\end{aligned}$$

By (6), $\hat{L}(\boldsymbol{\alpha}^{(t)}; \mathbf{x}^{(t)}) - (\boldsymbol{\epsilon}^{(t)})^\top \boldsymbol{\alpha}^{(t)} \leq \hat{L}(\boldsymbol{\alpha}^*; \mathbf{x}^{(t)}) - (\boldsymbol{\epsilon}^{(t)})^\top \boldsymbol{\alpha}^*$, and hence if the events $\tilde{E}, E_t$ hold,

$$\begin{aligned}
&(\boldsymbol{\epsilon}^{(t)})^\top \boldsymbol{\alpha}^{(t)} + \sum_{i=1}^{m} \left(\Delta_L \sqrt{\frac{1}{2n_i^{(t)}} \log \frac{m^2 T^2}{2\tilde{\delta}}} + \frac{\Delta_\kappa}{n_i^{(t)}} \right) \alpha_i^{(t)} \\
&\geq L(\boldsymbol{\alpha}^{(t)}) - L(\boldsymbol{\alpha}^*). \qquad (17)
\end{aligned}$$

We have

$$\begin{aligned}
&(\boldsymbol{\epsilon}^{(t)})^\top \boldsymbol{\alpha}^{(t)} + \sum_{i=1}^{m} \left(\Delta_L \sqrt{\frac{1}{2n_i^{(t)}} \log \frac{m^2 T^2}{2\tilde{\delta}}} + \frac{\Delta_\kappa}{n_i^{(t)}} \right) \alpha_i^{(t)} \\
&= \sum_{i=1}^{m} \left(\Delta_L \sqrt{\frac{\beta \log t}{2n_i^{(t)}} + \frac{\Delta_\kappa}{n_i^{(t)}}} + \Delta_L \sqrt{\frac{1}{2n_i^{(t)}} \log \frac{m^2 T^2}{2\tilde{\delta}}} + \frac{\Delta_\kappa}{n_i^{(t)}} \right) \alpha_i^{(t)} \\
&= \sum_i \left(\frac{\Delta_L}{\sqrt{n_i^{(t)}}} \left(\sqrt{\frac{\beta}{2} \log t} + \sqrt{\frac{1}{2} \log \frac{m^2 T^2}{2\tilde{\delta}}} \right) + \frac{2\Delta_\kappa}{n_i^{(t)}} \right) \alpha_i^{(t)} \\
&\leq \sum_i \left(\frac{\Delta_L}{\sqrt{n_i^{(t)}}} \left(\sqrt{\frac{\beta}{2} \log T} + \sqrt{\frac{1}{2} \log \frac{m^2 T^2}{2\tilde{\delta}}} \right) + \frac{\Delta_L}{\sqrt{n_i^{(t)}}} \right) \alpha_i^{(t)} \\
&= \Delta_L \eta \sum_i \frac{\alpha_i^{(t)}}{\sqrt{n_i^{(t)}}},
\end{aligned}$$

where

$$\eta := \sqrt{\frac{\beta}{2} \log T} + \sqrt{\frac{1}{2} \log \frac{m^2 T^2}{2\tilde{\delta}}} + 1.$$

Substituting into (17), if the events $\tilde{E}, E_t$ hold,

$$\Delta_L \eta \sum_i \frac{\alpha_i^{(t)}}{\sqrt{n_i^{(t)}}} \geq L(\boldsymbol{\alpha}^{(t)}) - L(\boldsymbol{\alpha}^*).$$

Hence, in general (regardless of whether $\tilde{E}, E_t$ hold), denoting the indicator function of $\tilde{E} \cap E_t$ as $\mathbf{1}_{\tilde{E} \cap E_t} \in \{0, 1\}$,

$$\sum_i \frac{\alpha_i^{(t)}}{\sqrt{n_i^{(t)}}} \geq \frac{L(\boldsymbol{\alpha}^{(t)}) - L(\boldsymbol{\alpha}^*)}{\Delta_L \eta} \mathbf{1}_{\tilde{E} \cap E_t}.$$

Let

$$\Psi^{(t)} := \sum_{i=1}^{m} \psi(n_i^{(t)} - 1),$$

where $\psi(n) := \sum_{i=1}^{n} i^{-1/2}$. Recall that we pull arm i at time $t+1$ with probability $\alpha_i^{(t)}$. The expected increase of $\Psi^{(t)}$ is

$$\begin{aligned}\mathbb{E}\left[\Psi^{(t+1)} - \Psi^{(t)} \,\middle|\, \mathbf{x}^{(t)}\right] &= \sum_{i=1}^{m} \left(\psi(n_i^{(t)}) - \psi(n_i^{(t)} - 1)\right) \alpha_i^{(t)} \\ &= \sum_{i=1}^{m} \frac{\alpha_i^{(t)}}{\sqrt{n_i^{(t)}}} \\ &\geq \frac{L(\boldsymbol{\alpha}^{(t)}) - L(\boldsymbol{\alpha}^*)}{\Delta_L \eta} \mathbf{1}_{\tilde{E} \cap E_t}.\end{aligned}$$

Note that

$$\begin{aligned}\Psi^{(T)} &= \sum_{i=1}^{m} \psi(n_i^{(T)} - 1) \\ &\leq \sum_{i=1}^{m} \int_0^{n_i^{(T)}-1} \min\{\tau^{-1/2}, 1\} \mathrm{d}\tau \\ &\overset{(a)}{\leq} m \int_0^{m^{-1}\sum_{i=1}^{m} n_i^{(T)} - 1} \min\{\tau^{-1/2}, 1\} \mathrm{d}\tau \\ &= m \int_0^{T/m-1} \min\{\tau^{-1/2}, 1\} \mathrm{d}\tau \\ &\overset{(b)}{=} m \left(1 + \int_1^{T/m-1} \tau^{-1/2} \mathrm{d}\tau\right) \\ &= m \left(2\sqrt{\frac{T}{m} - 1} - 1\right),\end{aligned}$$

where (a) is because $a \mapsto \int_0^a \min\{\tau^{-1/2}, 1\} \mathrm{d}\tau$ is concave, and (b) is because $T \geq 40m + 1$, so $T/m - 1 \geq 1$. Therefore,

$$\begin{aligned}m \left(2\sqrt{\frac{T}{m} - 1} - 1\right) &\geq \mathbb{E}\left[\Psi^{(T)} - \Psi^{(m)}\right] \\ &= \sum_{t=m}^{T-1} \mathbb{E}\left[\Psi^{(t+1)} - \Psi^{(t)}\right] \\ &\geq \sum_{t=m}^{T-1} \mathbb{E}\left[\frac{L(\boldsymbol{\alpha}^{(t)}) - L(\boldsymbol{\alpha}^*)}{\Delta_L \eta} \mathbf{1}_{\tilde{E} \cap E_t}\right] \\ &\geq \frac{1}{\Delta_L \eta} \sum_{t=m}^{T-1} \left(\mathbb{E}\left[L(\boldsymbol{\alpha}^{(t)}) - L(\boldsymbol{\alpha}^*)\right] - \Delta_L \mathbb{P}((\tilde{E} \cap E_t)^c)\right) \\ &\overset{(c)}{\geq} \frac{1}{\Delta_L \eta} \sum_{t=m}^{T-1} \left(\mathbb{E}\left[L(\boldsymbol{\alpha}^{(t)}) - L(\boldsymbol{\alpha}^*)\right] - \Delta_L (\tilde{\delta} + m^2 t^{-2}/2)\right) \\ &\geq \frac{1}{\Delta_L \eta} \sum_{t=m}^{T-1} \mathbb{E}\left[L(\boldsymbol{\alpha}^{(t)}) - L(\boldsymbol{\alpha}^*)\right] - \frac{T\tilde{\delta}}{\eta} - \frac{m^2}{2\eta} \int_{m-1}^{T-1} t^{-2} \mathrm{d}t \\ &\geq \frac{1}{\Delta_L \eta} \sum_{t=m}^{T-1} \mathbb{E}\left[L(\boldsymbol{\alpha}^{(t)}) - L(\boldsymbol{\alpha}^*)\right] - \frac{T\tilde{\delta}}{\eta} - \frac{m^2}{2\eta(m-1)} \\ &\geq \frac{1}{\Delta_L \eta} \sum_{t=m}^{T-1} \mathbb{E}\left[L(\boldsymbol{\alpha}^{(t)}) - L(\boldsymbol{\alpha}^*)\right] - \frac{T\tilde{\delta}}{\eta} - \frac{m}{\eta},\end{aligned}$$

where (c) is by (14). Hence,

$$
\begin{aligned}
&\frac{1}{\Delta_L}\sum_{t=0}^{T-1}\mathbb{E}\left[L(\boldsymbol{\alpha}^{(t)})-L(\boldsymbol{\alpha}^*)\right]\\
&\le \frac{1}{\Delta_L}\sum_{t=m}^{T-1}\mathbb{E}\left[L(\boldsymbol{\alpha}^{(t)})-L(\boldsymbol{\alpha}^*)\right]+m\\
&\le \eta m\left(2\sqrt{\frac{T}{m}-1}-1\right)+T\tilde{\delta}+2m\\
&\overset{(d)}{=} m\left(2\sqrt{\frac{T}{m}-1}-1\right)\left(\sqrt{\frac{\beta}{2}\log T}+\sqrt{\frac{1}{2}\log\frac{mT^3}{2}}+1\right)+3m\\
&\overset{(e)}{\le} m\left(2\sqrt{\frac{T}{m}-1}\right)\left(\sqrt{\frac{\beta}{2}\log T}+\sqrt{\frac{1}{2}\log\frac{mT^3}{2}}+1\right)\\
&\le 2\sqrt{mT}\left(\sqrt{\frac{\beta}{2}\log T}+\sqrt{\frac{1}{2}\log\frac{mT^3}{2}}+1\right),
\end{aligned}
$$

where (d) is by substituting $\tilde{\delta}=m/T$, (e) is because $\sqrt{\frac{\beta}{2}\log T}\ge\sqrt{2\log 81}\ge 2.9$ and $\sqrt{\frac{1}{2}\log\frac{mT^3}{2}}\ge 2.5$ (recall that $T\ge 40m+1\ge 81$). Substituting into (13),

$$
\begin{aligned}
&\frac{1}{\Delta_L}\left(\mathbb{E}[L(\hat{P}^{(T)})]-L(\boldsymbol{\alpha}^*)\right)\\
&\le \frac{1}{\Delta_L T}\sum_{t=1}^{T}\mathbb{E}\left[L(\boldsymbol{\alpha}^{(t-1)})-L(\boldsymbol{\alpha}^*)\right]+\frac{4\Delta_\kappa}{3\Delta_L}\sqrt{\frac{\log m}{2T}}+\frac{\Delta_\kappa}{T\Delta_L}\\
&\le 2\sqrt{\frac{m}{T}}\left(\sqrt{\frac{\beta}{2}\log T}+\sqrt{\frac{1}{2}\log\frac{mT^3}{2}}+1\right)+\frac{2}{3}\sqrt{\frac{\log m}{2T}}+\frac{1}{2T}\\
&= \frac{1}{\sqrt{T}}\left(2\sqrt{\frac{\beta}{2}m\log T}+\sqrt{2m\log\frac{mT^3}{2}}+2\sqrt{m}+\frac{2}{3}\sqrt{\frac{\log m}{2}}+\frac{1}{2\sqrt{T}}\right)\\
&\le \frac{1}{\sqrt{T}}\Bigg(2\sqrt{\frac{\beta}{2}m\log T}+\sqrt{2m\log T^4}+\frac{2\sqrt{m\log T}}{\sqrt{\log 81}}\\
&\qquad+\frac{2}{3}\frac{\sqrt{m\log T}}{\sqrt{m\log(40m+1)}}\sqrt{\frac{\log m}{2}}+\frac{1}{2\sqrt{81}}\cdot\frac{\sqrt{m\log T}}{\sqrt{2\log 81}}\Bigg)\\
&= \sqrt{\frac{m\log T}{T}}\left(\sqrt{2\beta}+2\sqrt{2}+\frac{2}{\sqrt{\log 81}}+\frac{2}{3}\sqrt{\frac{\log m}{2m\log(40m+1)}}+\frac{1}{2\sqrt{81}}\cdot\frac{1}{\sqrt{2\log 81}}\right)\\
&\le \sqrt{\frac{m\log T}{T}}\left(\sqrt{2\beta}+2\sqrt{2}+\frac{2}{\sqrt{\log 81}}+\frac{2}{3}\sqrt{\frac{\log 2}{4\log 81}}+\frac{1}{2\sqrt{81}}\cdot\frac{1}{\sqrt{2\log 81}}\right)\\
&\le \sqrt{\frac{m\log T}{T}}\left(\sqrt{2\beta}+3.934\right)\\
&\le \sqrt{\frac{m\log T}{T}}\left(\sqrt{2\beta}+\frac{3.934}{2}\sqrt{\beta}\right)\\
&\le 3.382\sqrt{\frac{\beta m\log T}{T}}.
\end{aligned}
$$

This completes the proof of Theorem 2 (with an improved constant 3.382 instead of 4).